JSAT

Journal of Science and Agricultural Technology

e-ISSN 2730-1532, ISSN 2730-1524

J. Sci. Agric. Technol.
Vol. 1 | No. 1 | January - June 2020

https://www.tci-thaijo.org/index.php/JSAT

Journal of Science and Agricultural Technology

J. Sci. Agri. Technol. (2020) Vol. 1 (1)

JSAT

JSAT
Journal of Science and Agricultural Technology
e-ISSN 2730-1532, ISSN 2730-1524

EDITORIAL TEAM

e-ISSN 2730-1532, ISSN 2730-1524

Welcome message from Editor-in-Chief

It is my pleasure and great privilege to present to you the first issue of *Journal of Science and Agricultural Technology* (JSAT), the official journal of the Faculty of Science and Agricultural Technology, Rajamangala University of Technology Lanna (RMUTL), Thailand. This new peer-reviewed international journal promises to make a significant impact upon the field of science and agricultural technology from Thai and international researchers around the globe. The scope of science includes biology, chemistry, biochemistry, computer science, physics, material science, mathematics, statistics etc. while the scope of agricultural technology covers those manuscripts related to plant science, animal science, aquatic science, food science, biotechnology, applied microbiology, agricultural machinery, agricultural engineering, and related fields. The journal features a distinguished editorial board, which brings together a team of highly experienced specialists in science and agricultural technology researches. The JSAT is published twice yearly.

As an Editor-in-Chief, I am looking forwarding to working with all of you in your role as an author, reviewer or editor to provide the reader of JSAT with a new, well-constructed, informative, and educational journal. I am confident that authors and reviewers using the system of manuscript online submission and review via Thai journal online (Thaijo) will find it user-friendly and straightforward. The entire editorial board and I strongly encourage you to submit manuscripts to educate and support the growing field of science and agricultural technology. I would like to take this opportunity to express my sincere gratitude to those scholars of the editorial broad, those in the editorial office, and those administrative team of RMUTL led by Assoc. Prof. Seensiri Sa-Ngajit: acting the President of RMUTL, for their strongly supports.

(Assoc.Prof. Dr. Suntorn Wittayakun)
Editor-in-Chief
Journal of Science and Agricultural Technology

e-ISSN 2730-1532, ISSN 2730-1524

ABOUT THE JOURNAL

Journal of Science and Agricultural Technology (JSAT) publishes original research contributions covering science and agricultural technology such as:

• Natural and applied sciences: biology, chemistry, computer science, physics, material science and related fields. Papers in mathematics and statistics are also welcomed, but should be of an applied nature rather than purely theoretical.

• Agricultural technology: plant science, animal science, aquatic science, food science, biotechnology, applied microbiology, agricultural machinery, agricultural engineering and related fields.

Furthermore, the JSAT journal aims to span the whole range of researches from local to global application.

The JSAT is published two issues a year.
Issue 1: January - June
Issue 2: July - December

Submissions are welcomed from international and Thai institutions. All submissions must be original research not previously published or simultaneously submitted for publication or submitted to other journals. Manuscripts are peer reviewed using the double-blinded review system by at least 2 reviewers before acceptance. There is no publication or processing fee.

The journal financial support is provided by Rajamangala University of Technology Lanna, Thailand.

Editorial office:
Faculty of Science and Agricultural Technology,
Rajamangala University of Technology Lanna,
128 Huaykaew Rd., Changphuek, Muang, Chiang Mai, 50300 Thailand.
Tel/Fax: +665392 1444 Ext. 1506

CONTENTS

JSAT
Journal of Science and Agricultural Technology
Research Article
https://doi.org/10.14456/jsat.2020.1
e-ISSN 2730-1532, ISSN 2730-1524

The cloning of the MPER1 and PX3 peroxidase genes conferring bacterial blight disease resistance genes in cassava (*Manihot esculenta* (L.) Crantz)

Payungsak Rauyaree[1]*, Paranee Sawangsri[1], and Suphawadee Ngorian[1]

[1]Biotechnology Research and Development Office, Department of Agriculture, Rangsit-Nakhon Nayok Road, Thanyaburi District, Pathumthani, Thailand 12110.

***Corresponding author**: payungsak_r@yahoo.com*

Received November 26, 2019. Revised January 21, 2020; March 18 2020. Accepted March 22, 2020.

Abstract

Cassava bacterial blight, CBB caused by *Xanthomonas ampestris pv. manihotis* pv. *Manihotis* is an important outbreak of cassava bacterial disease in Thailand. Plant peroxidases play major roles in many physiology processes both abiotic and biotic stress including plant defense response against a bacterial pathogen. The objective of this research was to clone the peroxidase genes homologs in cassava variety Rayong 60 (MTAI 8), which is a disease-resistant variety against cassava bacterial blight by using polymerase chain reaction method. According to our results, two peroxidase genes homolog named *MPER1* (cationic peroxidase; GenBank Accession No. EF645823) and *PX3* (secretory peroxidase; GenBank Accession No. EF645824) in cassava MTAI8 genome were isolated and determined. The *MPER1* contains 1,211 nucleotide 2 exons and 1 intron with 73% similarity to the peroxidase gene in *Arabidopsis thaliana which* was the first plant to have its genome sequenced, and is a popular tool for understanding the molecular biology of many plant traits. The *PX3* contains 945 nucleotides 3 exons and 3 introns with 57% high similarity to peroxidase gene in *Arabidopsis thaliana*. The predicted amino acid sequence revealed a 98 and 134-amino acid for *MPER1* and *PX3*, respectively. Both of the genes showed conserved a domain of peroxidase genes (gene superfamilies) with other plant species. These genes will be useful as a molecular marker in selecting disease-resistant varieties and for further used as plant genetic improvement approach.

Keywords: cassava bacterial blight, CBB, MPER1, PX3

Introduction

Cassava (*Manihot esculenta* (L.) Crantz) is one of the most important crops, being one of the main sources of calories for more than one billion people mainly in poor countries worldwide especially in sub-Saharan Africa, Southeast Asia, South America and some Pacific Island nations (Cock, 1985; Wydra et al., 2004; Johana et al., 2017). Due to its characteristic of high protein level, this causes the crop more to biotic stress including cassava bacterial blight (CBB) (Chittoor et al., 1997). Cassava bacterial blight caused by *Xanthomonas campestris* pv. *Manihotis* (*Xam*) is considered the most important foliar and vascular bacterial disease for cassava causing the yield loss up to 92% and is regarded as one of the most limiting diseases of cassava production worldwide (Umemura and Kwano, 1983). CBB is usually controlled through host resistance (Paula et al., 2018).

Peroxidases are enzymes that catalyze the oxidation of molecules at the expense of (H_2O_2) recognizing a broad range of substrates. Plant peroxidase genes have been mostly involved in activities during wounding, disease resistance, and physiological stresses such as radiation, salinity, and pollution (Campa, 1991). Pareira et al. (2000) reported that peroxidases can act as catalysts for the polymerization of phenolic compounds to form lignin and suberin in the plant cell wall, which can act as a barrier to block the spread of the pathogen in the plant (Fritig et al., 1987).

Peroxidases were suggested to play an important role in CBB (Flood et al., 1995). The identification of peroxidases has been demonstrated in interactions between cotton and *X. campestris* pv. *Malvacerum* (Dai et al., 1996); rice and *X. oryzae* pv. *Oryzae* (Chittoor et al., 1997). Rauyaree et al. (2001) reported the identification of peroxidases in Thai rice resistant to *Pyricularia grisea*. Pareira et al. (2003) reported the identification and initialization of a cassava peroxidase gene fragment by PCR, MEPX1, and its polymorphisms among different cassava cultivars.

For screening of the susceptible and resistance characterization among cassava varieties compared with conventional breeding, peroxidases

https://doi.org/10.14456/jsat.2020.1

could be used as potential molecular markers that would provide the benefit of cost, rapid results and accurate. (Flood et al., 1995). Cassava variety used in this study was Rayong 60 (MTAI 8 in the germplasm collection) which was resistant to CBB. MTAI 8 in the germplasm collection is resistant to CBB, based on Flood et al. (1995), that classified MTAI 1 and MTAI 8 from Thailand are resistant cultivar to CBB at 4 scales. The objectives of this study were to isolate two peroxidase genes homologs in cassava bacterial blight disease (CBB) from Thai cassava Rayong 60 variety by PCR method.

Materials and methods

Cassava variety

Cassava variety used in this study was Rayong 60 (MTAI 8 in the germplasm collection) which was resistant to CBB. The cassava variety was developed by Rayong Field Crops Research Center, Department of Agriculture, Rayong Province, Thailand. Plants were grown for vegetative propagation and 4-week-old; leaves were collected and used for DNA isolation (NucleoSpin Plant L Kits, CLONTECH, Palo Alto, CA)

Polymerase chain reaction (PCR)

The deduced amino acid sequences of seven peroxidase genes from seven species including *Solanum tuberosum, Nicotiana tabacum, Hordeum vulgare, Oryza sativa, Pisum sativum, Spinacia oleracea,* and *Minihot esculenta* used in this study were compared using the Clustal W program (http://ebi.ac.uk/clustalW) to identify highly conserved regions. The two primers designed from highly conserved regions of the retrieved sequences for cationic peroxidase and secretory peroxidase genes in sense and antisense direction, respectively. PCR was carried out in 50 ul and contained genomic DNA, 2 mmol/l Mg2Cl, 10 mmol/l Tris-HCl (pH 8.3), 50 mmol/l KCl, 1.5 U Taq polymerase, 2 mmol/l of each dNTP, 0.5 umol/l of each primer (Ward medic Thailand). Primers sequences used in this study were indicated in tables 1 and 2. After an initial denaturation step for 2 min at 94°C, 30 amplification cycles were performed. Each cycle included denaturation at 94°C for 2 min, annealing 50°C for 1 min, extension 72°C for 1 min and a final extension 72 °C for 5 min, modified from Pareira et al. (2003).

Cloning and sequence analysis

PCR products of the expected sizes were cloned into pDrive® Cloning Vector according to the protocol described by the manufacturer (Qiagen, USA) (TransformAid™ Bacterial transformation kit, Life Science, USA). Plasmid DNA was obtained from QIAprep spin miniprep kit, Qiagen, Valencia, USA. Plasmid DNA harboring insert was analyzed and digested by *Eco*RI restriction enzyme (Figure 2); and sequenced using the BigDye® Terminator v3.1 Cycle Sequencing (Perkin-Elmer, CA, USA) on an ABI PRISM™ model 377 DNA sequencer. The primers used for sequencing reactions were SP6 (5'-CATTTAGGTGACACTATAG-3') or T7 (5'-GTAATACGACTCACTATAG-3') at the concentration of 3.2 pmole. The sequences were analyzed with DNAStar expert sequence analysis software, DNAStar, Inc, USA and compared against GenBank NCBI non-redundant sequence database (BlastN program) (Gapped BLAST VERSION 2.0, Altschul et al., 1997).

Gel electrophoresis

Following amplification, 5 µl of each PCR product was analyzed by electrophoresis in a 1% agarose gel and stained with ethidium bromide. The gels were visualized with UV light and photographed (Figure 1).

Table 1. Gene Specific Primers used to amplify Cationic peroxidase in PCR.

Primer Names	Nucleotide sequences
(1) PXC-1 **Forward Primers**	GC(AGCT)(AC)G(AGCT)GA(CT)(AT)(GC)(AGCT)GT
(2) PXC-1 **Reverse Primers**	(AG)TG(AGCT)A(AG)(AGCT)A(AG)(AGCT)CC(CT)TT
(3) PXC-2 **Forward Primers**	(CT)T(AGCT)GG(AGCT)(AC)G(AGCT) (AC)G(AGCT)GA(CT)
(4) PXC-2 **Reverse Primers**	CAT(CT)TT(AGT)ATCAT(AGCT)GC
(5) PXC2-1 **Reverse Primers**	(AG)TT(AGCT)CCCAT(CT)TT(AGT)ATCAT(AGCT)GC

https://doi.org/10.14456/jsat.2020.1

Table 2. Gene Specific Primers used to amplify the secretory peroxidase in PCR.

	Primers	Base sequences
(6)	PXS1 Forward Primers	GAGTTGGCAGAGAAGGATGC
(7)	PXS1 Reverse Primers	TGTGCACCTGAGAGAACCAC
(8)	PXS2 Forward Primers	GAGTTGGCAGAGAAGGATGC
(9)	PXS2 Reverse Primers	GTGTGCACCTGAGAGAACCA
(10)	PXS3 Forward Primers	GAGTTGGCAGAGAAGGATGC
(11)	PXS3 Reverse Primers	TGTGTGCACCTGAGAGAACC
(12)	PXS4 Forward Primers	GTGGAGGGATGTGAGAGCAT
(13)	PXS4 Reverse Primers	TGTGTGCACCTGAGAGAACC
(14)	PXS5 Forward Primers	GTGGAGGGATGTGAGAGCAT
(15)	PXS5 Reverse Primers	GTGTGCACCTGAGAGAACCA
(16)	PX Forward Primers	CGTCTCCACTTTCATGACTGC
(17)	PX Reverse Primers	GAAACCTACCGTGTGTGCACC

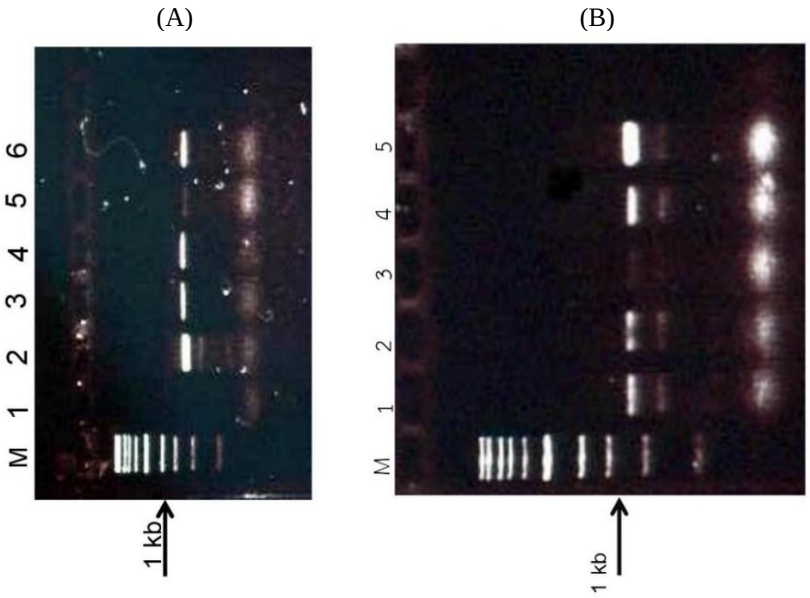

Figure 1. Agarose gel electrophoresis demonstrating the amplified PCR products derived from MTAI 8 (Rayong 60) as a template genomic DNA. (A) PCR bands obtained using gene specific primers cationic peroxidase (Lane 2 – 6); (B) PCR bands obtained using primers using gene specific primers secretory peroxidase in polymerase chain reaction (Lane 1 – 5). M = 1 kb DNA ladder.

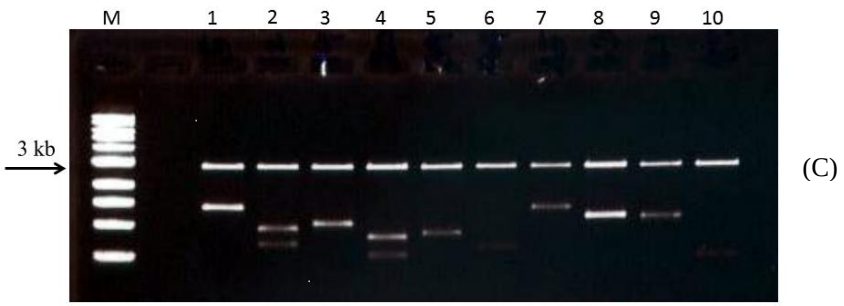

Figure 2. The cloned plasmid DNA harboring the DNA inserts was confirmed and by digestion with restriction enzymes *Eco*RI. (Lane 1 – 10); M = 1 kb DNA Ladder.

https://doi.org/10.14456/jsat.2020.1

Results and discussion

PCR reactions and Cloning

The PCR products were amplified from Rayong 60 genomic DNA using primer pairs (1-3), (6-7), (8-9), (10-11), (12-13) and (14-15). Two different sizes were cloned and cloned PCR product of 1,211 bp (*MPER1*, GenBank Accession No.EF645823) and 945 bp (PX3, GenBank Accession No.EF645824) showed sequence homology with 73% and 57% similarity to peroxidase gene in *Arabidopsis thaliana*, a small flowering plant that is widely used as a model organism in plant biology, respectively.

Nucleotide sequence analysis of the peroxidase genes

The nucleotide sequence of a 1,211 bp fragment containing the cationic peroxidase *MPER1* gene and a 945 bp fragment containing secretory peroxidase gene PX1 gene and its flanking regions were determined. For *MPER1*, a 293 bp open reading frame was obtained, encoding the enzyme which was comprised of 98 amino acid residues with a calculated molecular weight of 10.78 kDa. The deduced amino acid sequence of the Rayong 60 cationic peroxidase showed a high degree of identity to *Arabidopsis thaliana* peroxidase at 73% The fragment comprises of 2 exons and 1 intron. For *PX1*, a 403 bp open reading frame was obtained, encoding the enzyme which was comprised of 134 amino acid residues with a calculated molecular weight of 14.74 kDa. The deduced amino acid sequence of the Rayong 60 secretory peroxidase showed a high degree of identity to *Arabidopsis thaliana* peroxidases at 57%. The PX1 fragment comprises 3 exons and 3 introns.

Recently, Johana (2017) reported QTL that represents a first step in the dissection of the molecular mechanisms that govern CBB resistance in cassava and a new source of genes to be validated through different approaches. Furthermore, the resistance to CBB has been classified as a quantitative trait, the detection and localization on the genetic map of cassava QTL (Quantitative Trait Loci) conferring resistance to CBB would still useful for developing disease resistance lines. With the advance of gene methodologies like gene editing, the function of the interesting genes in CBB resistance would also be possible (Sander and Joung, 2014). Despite the fact that plants have evolved several mechanisms to defend themselves against pathogens, these mechanisms have solely been extensively studied in model plants. But the knowledge generated in cassava is relatively scarce. Further attempts might be involved with identifying new Thai cassava varieties that are more tolerance or resistance to CBB by both NBTs (New Breeding Techniques) and/or by transgenic approach. This result reported here might improve our understanding and knowledge regarding bacterial blight disease-resistant genes for CBB. *MPER1* and *PX1* could be useful as a marker for the identification of new resistant varieties.

GenBank Accession No. 645823 (*MPER1*)

```
   1 GTGGAGGGAT GTGAGAGCAT TAGAAAGGCT AAGGCATTGG TGGAGAGCAA GTGTCCTGGT
  61 GTTGTATCCT GTGCAGATAT TCTTGCAATT GCTGCCAGAG ATTATGTCCA CCTGGTATGC
 121 CTCTGCATTT CAATTCTTGA TATCCCCTAC TCAATCCTTA ATTAACTATT TCAAACTCTA
 181 GATCTTATCC CACTCAATCA AAACTTATTA ACAATTTGGA ATATATTGAT GGTAACAAAG
 241 TCCTATAAAT AATCCAAAGC ATAGGGCTGG TTTGTTGATA TAAGGGAAAT CAAATTTCTT
 301 GACTGTAGGT GAAAATATAT GTTGGGGTGC TCATACTCAT AATGCTTCCA AAGTAGAAAG
 361 GTGGAAAAAG GAAGATTGGT TTTGTCATTT TTGACAAAGT ATTTATAACA AAACAAACTC
 421 TTCTAAAAGG GCAAGAAAGT ATAAAAAATC ATTAAGTCCA TGTGATTTGA ACAGCTAGGT
 481 TATTTGTCCT TTGCTAGAAT CAATATCTCT ATGAAAGTCA AGAATATTAA TCAATTAATC
 541 CTTCCAAAAA TAGGACCAAT GCTGTGAAAA ACCAAATGCC TCATTCACTG GTAACATGAT
 601 GAGAGAACTA ATAGACAATA AGACTGGCAT TTGACTTGTA TTGGTTTTCT AAATGTCTCA
 661 TTCATTGGTA ACTGGATGTG GTCAATGATT TTTATTTTCT CAAAACTGTA CTCTTTTAGT
 721 TATTTTCTGT TAGGATAACA ATATTATTAT ATGACCCCAA TAATAATCAT TTGTATTATT
 781 ATTAAATTAG TAATTTATAT TCAAATTTCT ATATAAATTT TAGAAAAATT AACTATTTAG
 841 ATCATGCTAA ATTCATTAAT CGATCGTTCA GTTTTGAAAA ATATATTAAA ATATTTTTAA
 901 AATATTAAAA TATTTTTCAT AAATCTCTCT AAATTTTAAT TTATAAAACT CCTTTTTATA
 961 GACCTCTATT TTCTTCTAAA TAATCCTATA ATGGAGTGCT CTAATTCCAT ATGCTACATT
1021 TTCATGACGC AGGCAGGGGG ACCTTATTAC CAAGTGAAGA AAGGGAGATG GGATGGCAAA
1081 ATATCAATGG CATCAAGGGT ACCCTATAAT CTACCTCAAG CAAATTCAAC CATTGATCAA
1141 CTACTGAAGC TTTTCAATTC CAAAGGATTA ACACCACAAG ATCTAGTGGT TCTCTCAGGT
1201 GCACACAATC T

TRANSLATION =
        "VEGCESIRKAKALVESKCPGVVSCADILAIAARDYVHLAGGPYY
        QVKKGRWDGKISMASRVPYNLPQANSTIDQLLKLFNSKGLTPQD
        LVVLSGAHNL"
```

Figure 3. Nucleotide and 98 deduced amino acid sequence of the Rayong 60 Cationic peroxidase (*MPER1*) (GenBank Accession No. EF645823). Underlined represent exon parts of the coding regions.

https://doi.org/10.14456/jsat.2020.1

GenBank Accession No.EF645824 (*PX3*) ; Nucleotide sequence.

1 GTGATTCGTC TCCACTTTCA TGACTGCTTT GTCAGGGTTA GTGTTTTATT GTTTCTTCTT
61 AAGATTTGAT TTTCTTTTAG TTTGTAATTA TTTATTTCTT GTTAATAGGG ATGTGATGCT
121 TCGTTGTTGC TATCTTCGCC GAGTAACAAT GCGGAGAAAG ACCACCCGGA TAATCTTTCG
181 CTCGCCGGAG ATGGTTTTGA CACGGTGATC AAGGCAAAGG CTGCCGTTGA TAGTGTTTCT
241 CAATGCAGGA ACAAAGTTTC ATGTGCTGAT ATTCTGGCTC TTGCTACTAG AGATGTTGTA
301 TCTTTGGTAA GCAAGGTTTT TTCCCTTTAT TTTCGTTAAT TTTTTTTTTT TTAAAAATTA
361 TGGATTTTTT TTATTTCAAT TTTATATCTG ATGAGTTTGA AAATGGGTTG GATATTTTGA
421 GTATTCTATT TAATTGAATT TTATTGAAAT TCATATAATA TATATATGGT AGGAAATACT
481 TTATCCTCTT TAGTAGGTAT ATTTGGTATA ATGAATAAAT TTTACAAGTA TAATAAAGTT
541 GTGGAGCATG TGCATGATTA ATTAAATGAA ATGGAAATGC AGGCAGGAGG ACCATTTTAT
601 GAAGTGGAAC TAGGGAGGCG TGACGGGAGA ATATCAACAA AGGCAAGTGT TCAACACAAG
661 CTGCCAAGTG CTGACTTCAA TTTAGACCAG CTCAATTCTA TGTTCGCTTC ACTTGGCCTT
721 ACCCAAACTG ACATGATTGC TTTATCAGGT

TRANSLATION :

"VIRLHFHDCFVRGCDASLLLSSPSNNAEKDHPDNLSLAGDGFDT

VIKAKAAVDSVSQCRNKVSCADILALATRDVVSLAGGPFYEVEL

GRRDGRISTKASVQHKLPSADFNLDQLNSMFASLGLTQTDMIALSG"

Figure 4. Nucleotide and 134 deduced amino acid sequence of the Rayong 60 Secretory peroxidase (*PX3*) (GenBank Accession No. EF645824). Underlined represent exon parts of the coding regions.

```
Solanum_tuberosum       ------------------------------------------------------------
Nicotiana_tabacum       MASLKINAIVLFILVSLLIGSSSAQLSTGFYSKSCPKLYQTVKSAVQSAINKETRASL
Hordeum_vulgare         ---MASSSYTSLLVLVALVTAASAQLSPTFYDTSCPRALATIKSGVMAAVTSDPRASL
Oryza_sativa            -----MASSLSVAVLLCLAAAAAAQLSPTFYDTSCPRALATIKSAVTAAVNNEPRASL
Pisum_sativum           ------------------------------------------------------------
Spinacia_oleracea       -------VFLAIAIAIAIVGFAEAQLKLGYYSESCPKAEAIVESFVHQHIPHAQSLAAPL
Manihot_esculenta       ------------------------------------------------------------

Solanum_tuberosum       ---HFHDCFVNGCDASILLDQTATIDSEKTARPNNN---SARGFEVIDRIKSEVDKVCGR
Nicotiana_tabacum       LRLFFHDCFVNGCDGSLLLDDTSSFTGEKRAAPNVN---SARGFEVIDNIKSAVEKVCPG
Hordeum_vulgare         LRLHFHDCFVQGCDASVLLSG-----MEQNAIPNAG---SLRGFGVIDSIKTQIEAICKQ
Oryza_sativa            LRLHFHDCFVQGCDASVLLADTATFTGEQNALPNKN---SLRGFNVVDSIKTQLEGICSQ
Pisum_sativum           ---------------VLLNKTDTVVTEQEAFPNIN---SLRGLDVINRIKTAVENACPN
Spinacia_oleracea       LRMQFHDCFVRGCDASVLLDRTEAGNNDTEKTANPN--LTLRGFGFIDGVKSLLEEECPG
Manihot_esculenta       -RLHFHDCFVEGCDASILISTKPGSKELAEKDAEDNKDLRVEGCESIRMAKALVESKCPG
                                      :*:             .: .     .*   :   *: ::  *
                         Myr/Pho
Solanum_tuberosum       PVVSCADILXAAARDSVVALHGPTWEVELGRRDSTTASRTTANNDIPTPLMDLPALIDNF
Nicotiana_tabacum       -VVSCADILAVTARDSVVILGGPNWNVKLGRRDSRTASQSAANSGIPPATSNLNRLISSF
Hordeum_vulgare         -TVSCADILTVAARDSVVALGGPSWTVPLGRRDSIDANENEANTDLPGFNSSRAELEAAF
Oryza_sativa            -TVSCADILAVAARDSVVALGGPSWTVGLGRRDSTTASMDSANNDLPPPFFDLENLIKAF
Pisum_sativum           -TVSCADILALSAQISSILAQGPNWKVPLGRRDGLTANQSLANTNLPAPFNTLDELKAAF
Spinacia_oleracea       -VVSCADIIALVARDSVWTIGGPWWPVTTGRRDGRISNETEALQNIPPPFSNFSSLQTIF
Manihot_esculenta       -VVSCADILAIAARDYVHLAGGPYYQVKKGRWDGKISMASRVPYNLPQANSTIDQLLKLF
                          .******:   *:      ** : *  ** *.  :    .  .:*       *   *
                                     Peroxidase domain
Solanum_tuberosum       KKQG-LDEEDLVALSGAHT-----------------------------------------
Nicotiana_tabacum       SAVG-LSTKDMVALSGAHTIGQARCTSFRARIYNETNN------LDASFARTRQSNCPRS
Hordeum_vulgare         LKKGGLNTVDMVALSGAHTIGQAQCSTFRARIYGGDTN------INAAYAASLRANCPQT
Oryza_sativa            GDKG-FSVTDMVALSGAHTIGQAQCTNFRGRIYN-ETN------IDAGYAASLRANCPPT
Pisum_sativum           AKQG-LTPTDLVALSGAHTFGRSHCSLFVDRLYNFSNTGKPDPSLNTTYLQELRKTCPK-
Spinacia_oleracea       ASKG-LDLKDLVLLSGAHTIGVAHCPSFSERLYNFTGRGYGQDPSLDSEYATNLMTRKCT
Manihot_esculenta       NSKG-LTPQDLVVLSGAHTVGF-----------------------------------------
                            * :   *:* ******

Solanum_tuberosum       ------------------------------------------------------------
Nicotiana_tabacum       SGSGDNNLAPLDLQTPNKFDNNYFKNLVDKKGLLHSDQQLFNGGSADSIVTS--YSNNPS
Hordeum_vulgare         VGSGDGSLANLDTTTANTFDNAYYTNLMSQKGLLHSDQVLFNNDTTDNTVRN--FASNPA
Oryza_sativa            AGTGDSNLAALDTTTPYSFDTAYYSNLLSNKGLLHSDQVLFNGNSTDNTVRN--FASNRA
```

Figure 5. Deduced amino acid sequences of peroxidase genes indicating conserved domain from various plant species including *Manihot esculenta*. Greenbox represents peroxidase domain (DLVVLSGAHTVGF) from various plant species analyzed by Clustal W program (http://ebi.ac.uk/clustakw).

https://doi.org/10.14456/jsat.2020.1

Conclusion

The cassava variety Rayong 60 exited two peroxidase genes named Cationic peroxidase (*MPER1*) and Secretory peroxidase (*PX3*). Cationic peroxidase (*MPER1*) and Secretory peroxidase (*PX3*) which were considered as gene families contain 1,211 and 945 nucleotide in lengths, respectively. Both of the genes were deposited under GenBank Accession Numbers EF645823 and EF645824 respectively at the NCBI database. *MPER1* contains 2 exons and intron that showed sequence high homology with peroxidase gene in Arabidopsis (*Arabidopsis thaliana*) at 73% and *PX3* contains 3 exons and 3 introns that showed sequence high homology with peroxidase genes in *A. thaliana* at 57%. Both genes exhibited conserved domain with peroxidase gene superfamilies in other plant species. *MPER1* and *PX1* were confirmed from the total similarity of the peroxidase conserved sequence DLVVLSSGAHTV and GPVVSC for Myr/Pho (myristic acid/polyhydroxyoctanoate) peroxidase enzyme. The two peroxidase genes can be used as potential molecular markers for screening varieties against CBB.

Acknowledgements

The authors thank Rayong Field Crops Research Center, Department of Agriculture for enabling Cassava variety Rayong 60 (MTAI8 in the germplasm collection). This research funding was supported by the Department of Agriculture, Thailand.

References

Altschul, S.F., Madden, T.L., Shaffer, A.A., Zhang, Z., Zhang, J., Miller W., and Lipman,D.J. 1997. Gapped BLAST and PSI-BLAST: A new generation of protein database search program. Nucleic Acids Res. 25: 3389-3402.

Campa, A.1991. Biological roles of plant peroxidase: known and potential function. In: Everse, J., Everse, K.E., and M.B. Grisham, (ed). Peroxidases in Chemistry and Biology. Florida: CRC Press. pp. 25-50.

Chittoor, M., Leach, J.E., and White. F.F. 1997. Differential induction of a peroxidase gene family during infection of rice by *Xanthomonas oryzae* pv. Oryzae. Mol. Plant-Microbe Interact. 10: 861-871.

Cock, J.H. 1985. Cassava: new potential for a neglected crops. Boulder, CO : West View Press. 192 pp.

Dai, G.H., Nicole, M., Andary, C., Martinez, C., Bresson, E., Boher, B., Daniel, J.F., and Geiger, J.P. 1996. Flavonoids accumulate in cell walls, middle lamellae and callose-rich papillae during and incompatible interaction between *Xanthomonas campestris* pv. *malvacearum* and *cotton*. Physiol. Mol. Plant Pathol. 49: 285-306.

Flood, J., Cooper, R.M., Deshappriya N., and Day, R.C. 1995. Resistance of cassava (*Manihot esculenta*) to *Xanthomonas* blight *in vitro* and in planta. Aspects Appl. Biol. 42: 277-284.

Fritig, B., Kauffmann, S., Dumas, B., Geoffroy, P., Kopp, M., and Legend, M. 1987. Mechanism of the hypersensitivity response of plants. In: Evered, D. and Hermett, S. (ed). *Plant resistance to viruses*. UK: Wiley Press. pp. 92-108.

Johana, C. S. S., Rubén, E., Mora, M., Boby, M., Jens, L., Fabio, A., Gómez, Cano., Agim, B., and Camilo, E. L. C. 2017. Major Novel QTL for Resistance to Cassava Bacterial Blight Identified through a Multi-Environmental Analysis. Front Plant Sci. 8:1169. 1-13.

Paula, A. D.T., Mariana, H. C., Juan C. O. C., Adriana, M. C., Mónica, A. P., Valerie, V., Paul, C. A., and Camilo, E. L. C. 2018. The overexpression of RXam1, a cassava gene coding for an RLK, confers disease resistance to *Xanthomonas axonopodis* pv. *manihotis*. Planta. 247(4): 1031–1042.

Pereira, L.F., Goodwin, P.W., and Erickson, L. 2003. Cloning of a peroxidase gene from cassava with potential as a molecular marker for resistance to bacterial blight. Braz Arch Biol. 46(2): 149-154.

Pereira, L. F., Goodwin P. H., and Erickson, L. E. 2000. Peroxidase activity during susceptible and resistant interactions between cassava (*Manihot esculenta*) and *Xanthomonas axonopodis* pv. *manihotis* and *Xanthomonas cassavae*. J. Phytopathology. 148: 575-577.

Rauyaree, P., Choi, W., Fang, E., Blackmon, B., and Dean. R.A.2001. Genes expressed during early stages of infection with the rice blast fungus *Magnaporthe grisea*. Mol. Plant. Pathol. 2(6): 347-354.

Sander J. D., and Joung J. K. 2014. CRISPR-Cas systems for genome editing, regulation and targeting. Nat. Biotechnol. 32: 347–355.

Umemura, Y., and Kawano. K. 1983. Field assessment and inheritance of resistance to cassava bacterial blight. Crop Sci. 23: 1127-1132.

Wydra, K., Zinsou, V., Jorge V., and Verdier, V. 2004. Identification of pathotypes of *Xanthomonas axonopodis* pv. *Manihotis* in Africa and detection of quantitative trait loci and markers for resistance to bacterial blight of cassava. Phytopathology. 94(10): 084-1093.

JSAT
Journal of Science and Agricultural Technology
Research Article
https://doi.org/10.14456/jsat.2020.2
e-ISSN 2730-1532, ISSN 2730-1524

Influence of different extraction solvents on antioxidant and antityrosinase activities of *Morus alba* Linn. leaf extract.

Wachira Yodthong[1], Suraphon Chaiwongsar[1], Penpicha Wanachantararak[2], Yanee Keereeta[1], Watee Panthuwat[1], Benjaporn Saovapha[3], Tanongsak Sassa-deepaeng[1]*

[1]Agricultural Biochemistry Research Unit, Faculty of Science and Agricultural Technology, Rajamangala University of Technology Lanna, Lampang, Thailand
[2] Dentistry Research, Faculty of Dentistry, Chiang Mai University, Chiang Mai, Thailand
[3] Boromrajonani College of Nursing Nakorn Lampang, Lampang, Thailand

***Corresponding author**: nai.rmutl@gmail.com
Received January 21, 2020. Revised February 9, 2020; March 23, 2020. Accepted March 23, 2020.

Abstract

The objective of this study was to investigate the impact of different extraction solvents such as hexane, benzene, ethyl acetate, acetone, ethanol, and water on antioxidant and antityrosinase efficiency of mulberry leaf extract. The sample was extracted from leaves by maceration method. The obtained extract was filtered and evaporated to dryness by using the rotary evaporator prior to measuring the total phenolic content, flavonoid content, antioxidant activity, antityrosinase activity, and morin content in triplicate. The results indicated that the highest antioxidant activity was found in ethyl acetate (EA) fraction of CM60 with ABTS value of 57.8 ± 7.7 % inhibition and DPPH value of 58.2 ± 0.7 % inhibition that were positively related to its phenolic content (36.9 ± 1.3 μg GAE/mg DW). Interestingly, The highest antityrosinase activity was found in acetone fraction of CM60 which inhibited tyrosinase activity by 3.0 ± 0.1 μg KE/mg DW that was positively related to its flavonoid content (32.71 ± 0.1 μg QE/mg DW) and was related to its highest morin content (0.71 ± 0.01 μg/mg DW) measured using HPLC. The present results indicated that the EA fraction of CM60 possessed the highest antioxidant property related to its phenolic content, and the acetone fraction showed the highest antityrosinase activity related to its flavonoid content especially morin which is tyrosinase inhibitor. Both fractions of *M.* alba were potential candidates for skin protector from oxidative damage and skin-whitening agent development. Further studies are necessary to formulate the compounds responsible for antioxidant and antityrosinase properties and to investigate antityrosinase properties *in vivo* prior to transferring technology to communities.

Keywords: mulberry, antioxidant, antityrosinase, solvent extraction

Introduction

Melanins are multifuctional polymers that are found in animals, plants, arthropods, bacteria, and fungi (Solano, 2014). They are classified into 3 forms, including eumelanin, pheomelanin, and neuromelanin. Eumelanin is the dominant form of melanin found in human melanocytes which plays important role in camouflage, thermoregulation and photoprotection of the skin against ultraviolets (Nasti and Timares, 2015; Ulbing et al., 2019). However, the over-exposure in sunlight lead to promoting synthesis of melanin resulted presenting of unpleasant skin color (Yun et al., 2015; Ribeiro et al., 2015). In addition, this excessive melanin synthesis and deposition in skin may cause melasma, freckles, lentigo and geriatric pigment spot lead to may not pursuit of most Thai women (Yun et al., 2015; Ya et al., 2015). Although numerous synthetic chemicals, such as hydroquinone and some derivatives, revealed high effective in skin lightening and in treatment of pigmentation disorders through inhibit melanin production and through decreasing the number of melanocytes, these can also lead to skin irritation and has been reported as carcinogen and mutagen (Agorku et al., 2016; McGregor, 2007; Parvez et al., 2006). It is important to find novel plant-based compounds which are safe and effective to overcome this side effects. Additionally, some active compounds from plants also showed as high potential antioxidants which are important in prevention of oxidative process in melanin production.

Mulberry (*Morus alba* L.), belonging to the Moraceae family, is a deciduous plant which is widely distributed in Thailand regarded as nutritious fruit for human, forage and silkworms. The leaves, twigs, and root barks have been used in medicine recipes to treat diabetes (Ranjan et al., 2017; Riche et al., 2017), diabetic nephropathy (Sheng et al., 2018), obesity (Kim, 2017; Chang et al., 2016), antioxidant (Kim and Lee, 2017; Bae and Suh, 2007), anti-dopaminergic (Hussain et al., 2017; Yadav and Nade,

https://doi.org/10.14456/jsat.2020.2

2008), atherosclerosis, and cancer (Hashemi and Khadivi, 2020; Chon et al., 2009). It was also found that numerous flavonoids, the most water-insoluble compounds, were the main active constituents of mulberry, including morin, resveratrol, quercetin, and quercetin derivatives (Chauhan et al., 2013; Sun et al., 2011). To achieve specific active compounds, various solvents with different polarities were employed in mulberry leaf extraction, including hexane, benzene, ethyl acetate, acetone, ethanol and water.

In this study, to obtain the most potent tyrosinase and oxidative inhibitory fraction, the impact of different polarity of solvents on antioxidant and antityrosinase activities of *Morus alba* Linn. leaf extract were investigated.

Materials and methods

Plant materials

The mature leaves of mulberry var. Chiangmai 60 (CM60) were collected randomly from 10 plants on May 7th, 2018 as recommended by Zou et al. (2012) in Rajamangala University of Technology Lanna Lampang (18.367053, 99.596299), Mueang Lampang District, Lampang, Thailand and then authenticated by an herbalist from Rajamangala University of Technology Lanna (RMUTL) whereas var. Buriram 60 (BR60) and Sakhonnakhon 75 (SN75) were available in the same manner on May 9th, 2018 as the voucher specimen from Queen Sirikit Sericulture Center Chiang Mai (18.903564, 99.013597) San Sai District, Chiang Mai, Thailand.

Sample preparation

Upon arrival, 500 mg of fresh sample was washed with tap water followed by distilled water prior to drying in hot air oven at 55 °C until constant weight. The dried sample was ground by using electric blender is obtained. Fine powder was collected by using 20-mesh sieves before stored at -20 °C for further analyses.

Sample Extraction

Extraction was conducted according to the sequential extraction method using different solvents including hexane, benzene, ethyl acetate, acetone (from RCI Labscan, Bangkok, Thailand), ethanol (from Liquor Distillery Excise Department, Bangkhla, Thailand) and water. Each solvent extraction was performed in triplicate as described by Thavamoney et al. (2018) with some modifications. The 10 g of mulberry powder was immersed in 250 mL of solvent at ambient temperature and was agitated at 180 rpm assisted by an orbital shaker for 180 min twice a day and then filtered. The remaining residue was subjected to re-extraction. The filtrates of each solvent were pooled and concentrated by using a rotary evaporator, while water filtrate was dried by using a freeze dryer.

ABTS assay

The ABTS free radical-scavenging activity was examined according to the modified method described by Sassa-deepaeng et al. (2017). The 7.0 mM ABTS (Sigma–Aldrich, Steinheim, Germany) aqueous solution and 2.45 mM Potassium persulfate (VolChem, Shantou Xilong Chemical Plant Co Ltd., China) was mixed and incubated at the ambient temperature for 16 hours in the dark to generate pre-formed radical cation $ABTS^{+}$. The working solution was diluted with DI water to absorbance values between 0.8±0.1 at 734 nm. The reaction was started by adding 20 µL of various concentrations (125, 250, 500, 1000 µg/mL) of samples to 980 µL of the working solution and then incubated at the ambient temperature for 30 min in the dark. The unpaired electrons were sequestered by antioxidants in the sample resulted the test solution turned into colorless. The measurement was performed against the bank at 734 nm using V-1200 spectrophotometer (Dshing Instrument Co., Ltd., China) with UV-Professional analysis software. The percentage of inhibition of antioxidant was calculated using the equation:

$$\% \text{ inhibition} = [(A_c - A_s)/A_c] \times 100$$

Where A_c was the absorbance of the control and A_s was the absorbance of the reaction mixture.

The linear curves were constructed by plotting the percentage of inhibition against the concentration in µg/mL ($R^2 = 0.99$).

DPPH assay

The 2,2-diphenyl-1-picrylhydrazyl hydrate (DPPH) radical-scavenging activity was examined using modified method described by Sassa-deepaeng et al (2019). DPPH (Sigma–Aldrich, Steinheim, Germany) solution (oxidized form) was prepared in absolute ethanol to get final absorbance of 0.8 ± 0.1 at 517 nm. One hundred µL of various concentrations (125, 250, 500, 1000 µg/mL) of samples were mixed with 900 µL of DPPH radical solution and then incubated at the ambient temperature for 30 min in the dark. The antioxidant of the sample, which can donate an electron to DPPH radical contributed in solution color develop into yellow. The solution was measured against the bank at 517 nm using V-1200 spectrophotometer (Dshing Instrument Co., Ltd., China) with UV-Professional analysis software.

https://doi.org/10.14456/jsat.2020.2

The percentage of inhibition of antioxidant was calculated using the equation:

$$\% \text{ inhibition} = [(A_c-A_s)/A_c] \times 100$$

Where A_c was the absorbance of the control and A_s was the absorbance of the reaction mixture.

The linear curves were constructed by plotting the percentage of inhibition against the concentration in µg/mL ($R^2 = 0.99$).

Total phenolic content

The total phenolic content (TPC) was examined using the Folin-Ciocalteu (FC) colorimetric method. Twenty µL of various concentrations (125, 250, 500, 1000 µg/mL) of the extract was added to 100 µL of FC (Merck, Damstadt, Germany) reagent in 1,980 µL of DI water and then was incubated for 5 min at the ambient temperature. Afterward, 300 µL of 7% of Na_2CO_3 (Univar, Ajax Finechem, Australia) was added and incubated again for 60 min at the ambient temperature in the dark, the absorbance of the solution was measured at 765 nm using V-1200 spectrophotometer with UV-Professional analysis software. TPC quantitation was performed in triplicate. The gallic acid at different concentrations was used to generate the calibration curve ($R^2 = 0.99$). The TPC was expressed as microgram gallic acid (Bio Basic Inc., Ontario, Canada) equivalent (GAE) per milligram dry weight (Sassa-deepaeng et al., 2017).

Flavonoid content

The flavonoid content (FC) was examined using aluminum trichloride ($AlCl_3$) colorimetric method with some modified by Sassa-deepaeng et al. (2019). Twenty µL of various concentrations (125, 250, 500, 1000 µg/mL) of the extract was added to 380 µL of DI water followed 100 µL of 5% $NaNO_2$ (Univar, Ajax Finechem, Australia) and incubated for 5 min at the ambient temperature. Afterward, 100 µL of 10% $AlCl_3$ (Lobachemie, Mumbai, India) was added and was incubated again for 6 min at the ambient temperature. At the final step, 400 µL of 1M NaOH (Merck KGaA, Darmstadt, Germany) was added and then incubated for 15 min in the dark. The absorbance was measured at the wavelength of 415 nm using V-1200 spectrophotometer with UV-Professional analysis software. The flavonoid quantitation was carried out in triplicate and the FC was expressed as microgram quercetin (Sigma–Aldrich, Steinheim, Germany) equivalent (QE) per milligram dry weight.

Antityrosinase activity

The antityrosinase activity was performed according to the method described by Momtaz et al. (2008). The standard inhibitor and extracts (400 µg/mL) were dissolved in ethanol (Liquor Distillery Excise Department, Bangkhla, Thailand) and then diluted in 50 mM dibasic sodium phosphate buffer, pH 6.6. The extracts were firstly pre-tested at one concentration of 400 µg/mL for their inhibitory effect on tyrosinase. Afterwards, the samples which possessed the inhibitory effect were selected for further study in various dilutions ranged from 3.125 to 800 µg/mL. Kojic acid was used as positive control. The 70 µL of each extract was mixed with 30 µL of tyrosinase (333 U/mL) in 96-well microplate (Sterilin, Sterilin Limited, U.K.) and incubated for 5 min at the ambient temperature. Afterward, 110 µL of substrates (4 mM L-DOPA) was added to each well. The mixtures were then incubated for 30 min at the ambient temperature in the dark. The amount of dopachrome was measured at the wavelength of 492 nm using microplate reader (BIOBASE-EL10, Biobase Biodustry (Shandong) Co., Ltd., China). The percent inhibition of tyrosinase was calculated as the following equation:

$$\%\text{Tyrosinase inhibition} = [(A-B)-(C-D)/(A-B)] \times 100$$

Whereas,
A = absorbance of blank solution with tyrosinase
B = absorbance of blank solution without tyrosinase
C = absorbance of sample solution with tyrosinase
D = absorbance of sample solution without tyrosinase

HPLC apparatus and conditions

The morin content was determined by and in-house validated HPLC method on Hitachi CM-5000 Chromaster series (Chromaster, Hitachi, Japan) equipped with a 5110 pump, 5260 autosampler, 5310 column oven and 5430 diode array detector. The separation was performed on a Purospher® STAR RP-18 endcapped (250 mm x 4.6 mm i.d., 5 µm) column (Merck KGaA, Damstadt, Germany). The elution was conducted on isocratic solvent system using 0.1% phosphoric acid in acetonitrile (1:9) as mobile phase, filtered through a 0.45 µm Nylon membrane filter (Merck KGaA, Darmstadt, Germany) and sonicated for 10 min before use; flow rate of 1.0 mL/min for 10 min with controlled temperature at 25°C. DAD detector was set at the wavelength of 252 nm. The injection volume of samples and standards was 10 µL.

Statistical analysis

The data were analyzed using tool pack of the Microsoft Excel 2016 software. (Microsoft Corporation., CA, USA). One-way analysis of

https://doi.org/10.14456/jsat.2020.2

variance and the LSD range test were used to determine significant differences and the differences at $p < 0.05$ were considered significant.

Results and discussion

Sequential extraction procedures and solvents are the critical step which is responsible for dissolving the endogenous active compounds from mulberry leaves. To achieve the highest yield of active compound from sample, the different polarity of solvents (Reichardt, 2003) including hexane, benzene, ethyl acetate, acetone, ethanol and water with the polarity of 0.009, 0.111, 0.228, 0.355, 0.654, and 1.00 were used. Thus, due to the fundamental principle of solubility, active compounds in samples can be extracted by using appropriate solvents. The yield obtained from the extraction is shown in Figure 1.

The percent extraction yield in each of the mulberry variety up to 100% as indicated in Figure 1. The maximum yield was ethanolic extract of BR60 (47.5 ± 8.8), following of SN75 and of CM60, respectively, while the minimum extraction yield was found in acetonic extracts of BR60 (4.5 ± 1.5), following that of CM60 and SN75, respectively. It can be suggested that the major phytochemicals in mulberry leaves were mostly high in polarity as indicated by Andallu et al. (2014), and Zhang et al. (2010). Interestingly, the color of hexane extract was yellow with oily odor, while of the others were dark-greenish without oily smell. The possible explanation for this observation was the presence of lipid or lipophilic compound in hexane fraction. However, the result was not indicated which fractions possessed the active gradient. Therefore, ABTS assay for assessing the antioxidant activity of each extract was firstly conducted.

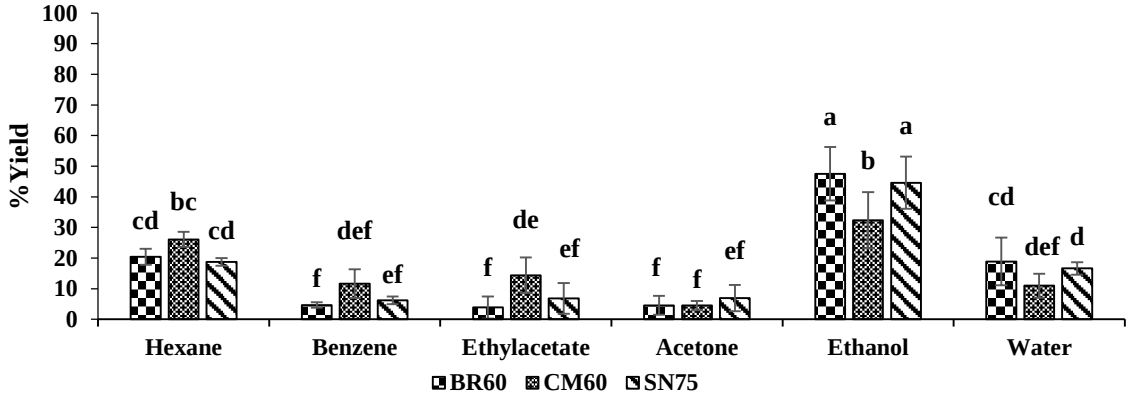

Figure 1. Yield of various extract of mulberry leaves. The error bars represent the standard deviation of mean. The different letters indicate significant difference ($p < 0.05$).

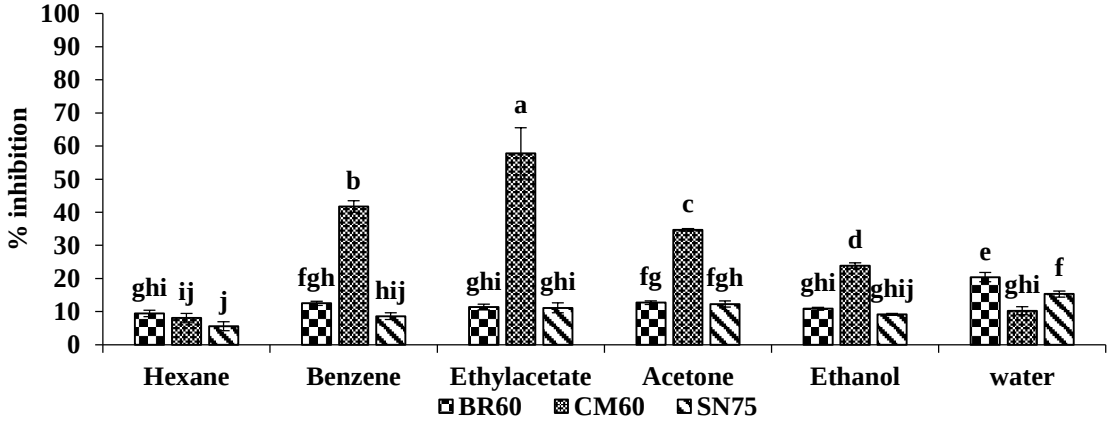

Figure 2. ABTS assay for assessing the antioxidant activity of *M. alba* (CM60, BR60 and SN75) leaf extracts in different solvents. The error bars represent the standard deviation of mean. The different letters indicate significant difference ($p < 0.05$).

https://doi.org/10.14456/jsat.2020.2

The free radical scavenging activity was screened in terms of the percentage inhibition of the ABTS radical cation by the antioxidants in sample. It was found that there was a significant variation in the percentage inhibition of the different solvent extracts (8.1 to 57.8 % inhibition) revealed in CM60 samples which were possessed the scavenging activity greater than BR60 and SN75 samples. The ranging inhibitory effect in the order of CM60 was ethyl acetate > benzene > acetone > ethanol as indicated in Figure 2. Concurrently, hexane extract had proved the most inefficient scavenger of the ABTS radical. It was confirmed that mainly antioxidant compounds were deposited in polar solvent extracts or the high-polarity components contributed to reducing power as documented by Li et al. (2017). Therefore, The DPPH scavenging activity was performed to insist upon the finding.

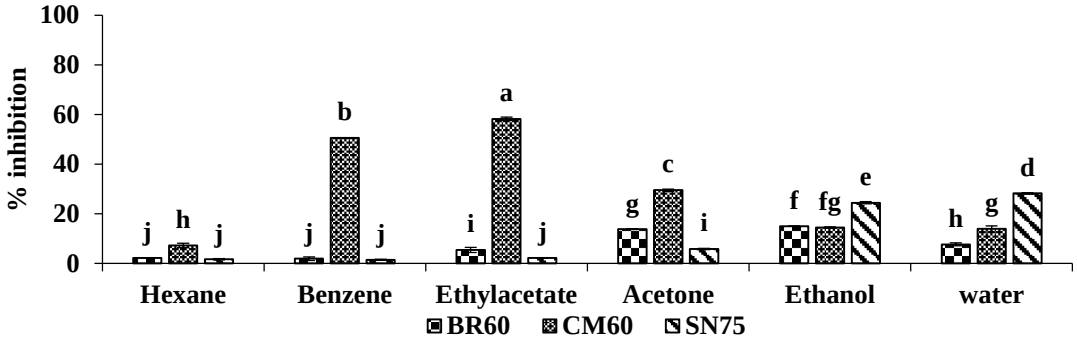

Figure 3. DPPH assay for assessing the antioxidant activity of *M. Alba* (CM60, BR60 and SN75) leaf extracts in different solvents. The error bars represent the standard deviation of mean. The different letters indicate significant difference ($p < 0.05$).

The DPPH scavenging activity was quantified in terms of the percentage inhibition of a pre-formed free radical by the antioxidants in sample. The similar pattern of the antioxidant inhibitory properties as mentioned in ABTS assay was obtained, but the values were slightly lower than ABTS assay as indicated by Saravanakumar et al. (2019) due to ABTS is more sensitive than DPPH when the sample consist of a large quantity of hydrophilic compounds. It was also found that the mostly DPPH radical scavenging activities of the CM60 extracts were greater than BR60 and SN75, and ranging in the order: ethyl acetate > benzene > acetone > water > ethanol > hexane as indicated in Figure 3. There was a significant variation in the percentage inhibition of the DPPH radical by the solvents (7.2 to 50.6 % inhibition). Again, ethyl acetate extract of CM60 showed the highest antioxidant capacity. Concurrently, all hexane extracts also had a considerably the lowest DPPH scavenging capacity. Interestingly, there was to be trend for the radical scavenging capacity of sample next to ethyl acetate seem to be slightly decreased following the increasing of solvent polarity. It was also found these characteristics in using less polarity solvents. Overall, the greatest DPPH radical scavenging activity was found in ethyl acetate extract of CM60. Therefore, the TPC assay was conducted to ascertain whether it was a factor which was related to the free radical scavenging activity.

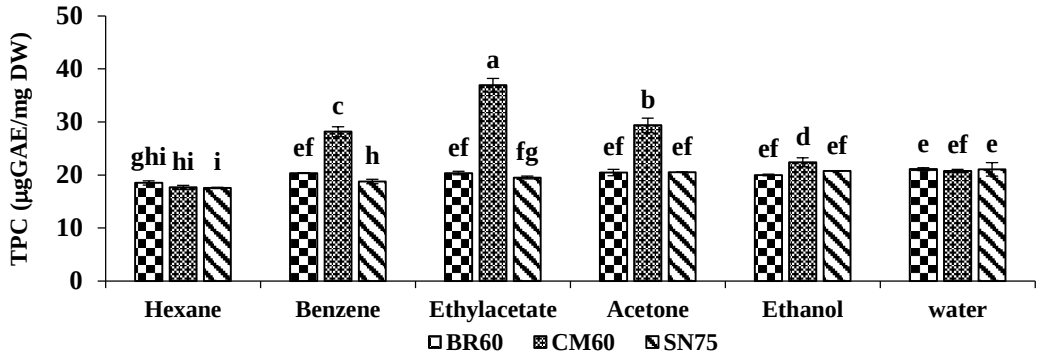

Figure 4. The total phenolic content of *M. alba* (CM60, BR60 and SN75) leaf extracts in different solvents. The error bars represent the standard deviation of mean. The different letters indicate significant difference ($p < 0.05$).

https://doi.org/10.14456/jsat.2020.2

Mulberry leaves were harvested in May as recommended by Zou et al. (2012) due to the highest total phenolic content was obtained. The TPC value was quantified by using the Folin–Ciocalteu reagent assay. It was found that the TPC values in three mulberry cultivars ranged from 17.55 to 36.92 µg GAE/mg DW, with the highest TPC content in ethyl acetate extract of CM60 and the lowest TPC content in hexanic extract of BR60 as shown in Figure 4. It can be suggested that the TPC was extracted at the appropriate polar as indicated by Abarca-Vargas et al. (2016). These findings were similar to report by Hao et al. (2018) who found a variation of the TPC of 24 Chinese mulberry leaves, ranging from 23.4 to 39.4 µg GAE /mg DW and similar the finding of Zou et al. (2012) who found a variation of the TPC of 6 Chinese mulberry leaves, ranging from 30.4 to 44.7 µg GAE/mg DW. In addition, acetonic extract and benzenic extract of CM60 were also revealed high TPC content. The values of phenolic content in this current study varied slightly compared to those literatures might be due to the geographical variation and flavonoid content. To investigate the influence of solvents on flavonoid content, the aluminum chloride was used for further study and presented in Figure 5.

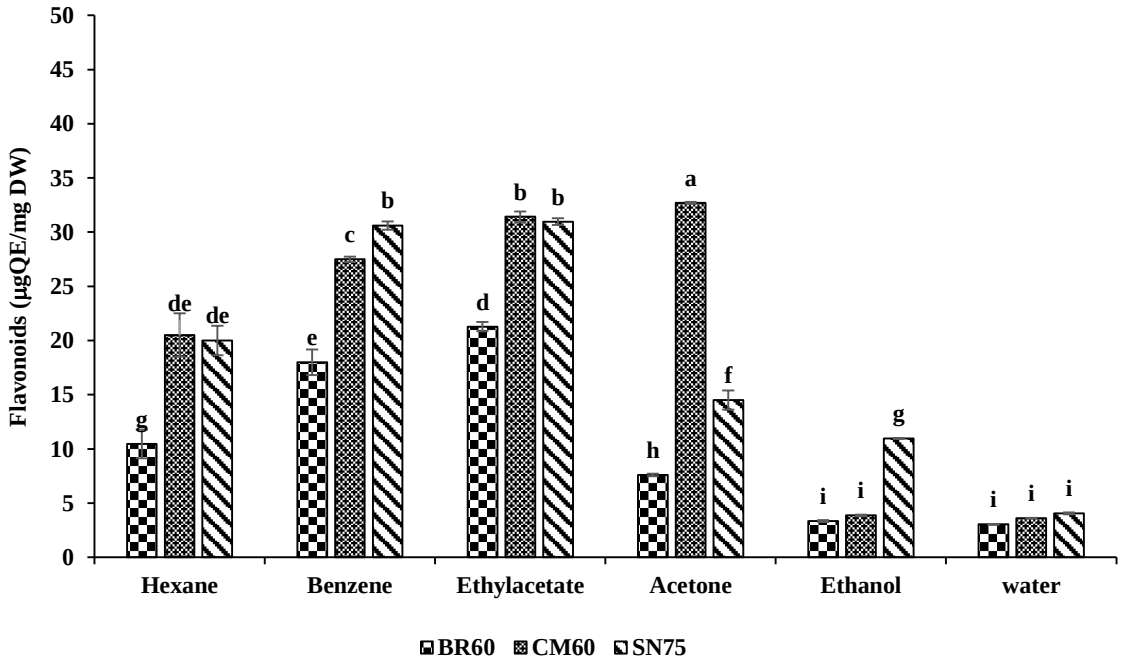

Figure 5. The flavonoid content of *M. alba* (CM60, BR60 and SN75) leaf extracts in different solvents. The error bars represent the standard deviation of mean. The different letters indicate significant difference ($p < 0.05$).

The flavonoid content in mulberry extracts was determined using aluminum chloride in a colorimetric method. It was found that the flavonoid values in three mulberry cultivars ranged from 3.0 to 31.4 µg QE/mg DW, with the highest flavonoid content in acetonic extract of CM60 and the lowest flavonoid content in all water extracts as shown in Figure 5. The flavonoid content was similar to report by Chang et al. (2011) who found the value of Taiwan mulberry leaf was 23.5 µg Rutin Equivalent /mg DW, but was slightly lower than the finding of Chauhan et al. (2013) who reported that flavonoid contents of mulberry varieties ranged from 40.7 to 165.6 µg GAE/mg DW. As indicated by Aryal et al. (2019), the genetic diversity, geographical variation, environmental factors, and season were also significantly affected the flavonoid content. To explore correlations of flavonoid and total phenolic content with their antioxidant activities, the correlation curve was generated and presented in Figure 6.

https://doi.org/10.14456/jsat.2020.2

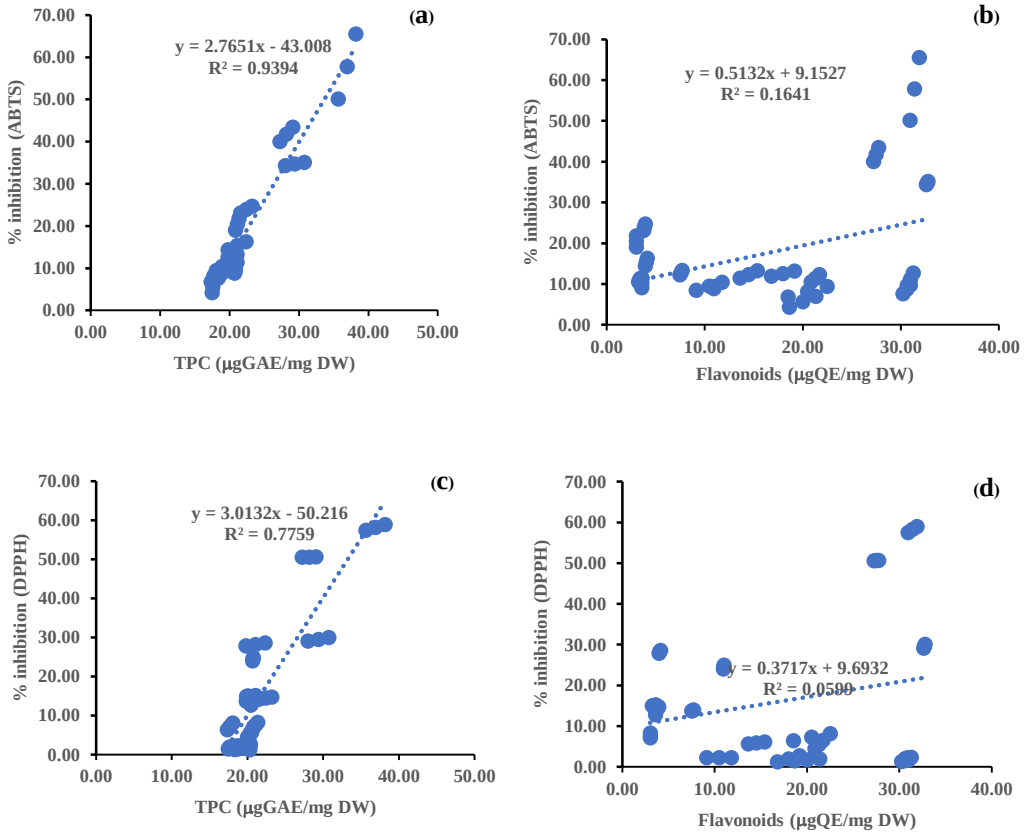

Figure 6. The correlation between (a) TPC content and % inhibition of ABTS, (b) Flavonoid content and % inhibition of ABTS, (c) TPC content and % inhibition of DPPH, and (d) Flavonoid content and % inhibition of DPPH.

It was found that the TPC content value was significantly correlated with percentage inhibition of ABTS ($R^2 = 0.9394$) and DPPH ($R^2 = 0.7759$) assays as presented in Figure 6, whereas the flavonoid content was not correlated with any antioxidant assay. The result was similar to the finding of Andarwulan et al. (2010) who found that the TPC value was highly correlated with DPPH and ABTS radical scavenging assays, but the flavonoid content was not correlated with those antioxidant activity. It could be associated with other pro-oxidant constituents or consisting of flavonoids which possessed low potential antioxidant property in the extracts. Interestingly, only the extracts of CM60 showed the correlation significantly with ABTS and DPPH assay. Thus, it can be suggested that CM60 extracts were trend to be high potential for cosmetics development. However, the results from antityrosinase assay were also need to be used for that purpose.

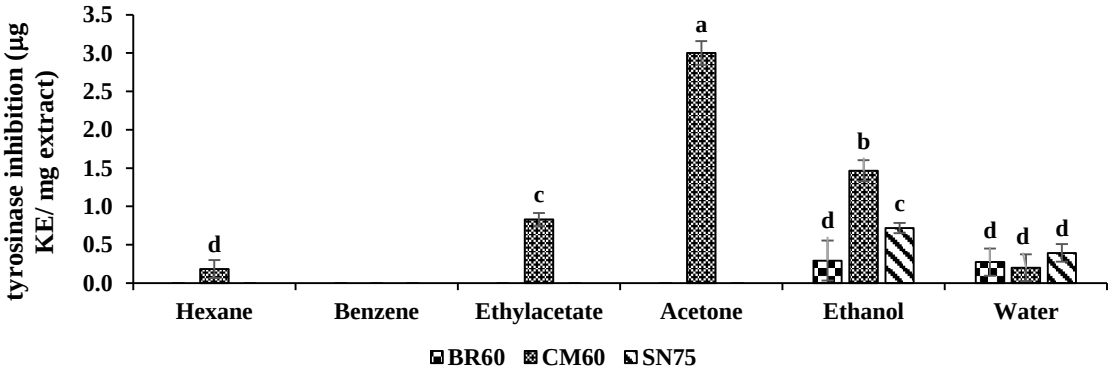

Figure 7. The antityrosinase inhibitory activity of *M. alba* (CM60, BR60 and SN75) leaf extracts in different solvents. The error bars represent the standard deviation of mean. The different letters indicate significant difference ($p < 0.05$).

https://doi.org/10.14456/jsat.2020.2

The antityrosinase inhibitory activity of different solvent extracts was determined in terms of the percentage inhibition of tyrosinase by various inhibitors in sample. It was found that the mostly inhibitory activities of CM60 extracts were greater than BR60 and SN75, and ranging in the order: acetone > ethanol > ethyl acetate as indicated in Figure 7. Unfortunately, the inhibitory activity was undetectable in any benzenic extracts and found only a small amount of activity in hexanic and water extracts. It was also found that there was a significant variation in the percentage inhibition of tyrosinase of CM60 extracts by the solvents (0.0 to 3.0 μg KE/mg extract). Interestingly, acetonic extract of CM60 showed the highest antityrosinase capacity. It was confirmed that mulberry leaf extract also possessed antityrosinase compound as it was found in twig and root (Chang et al., 2011). The antityrosinase activity might be involved the flavonoid composition such as morin as reports of Chang et al. (2011), and Zhang et al. (2016). Therefore, the HPLC method was conducted to further investigate the morin content in CM60 extracts and presented in Figure 8.

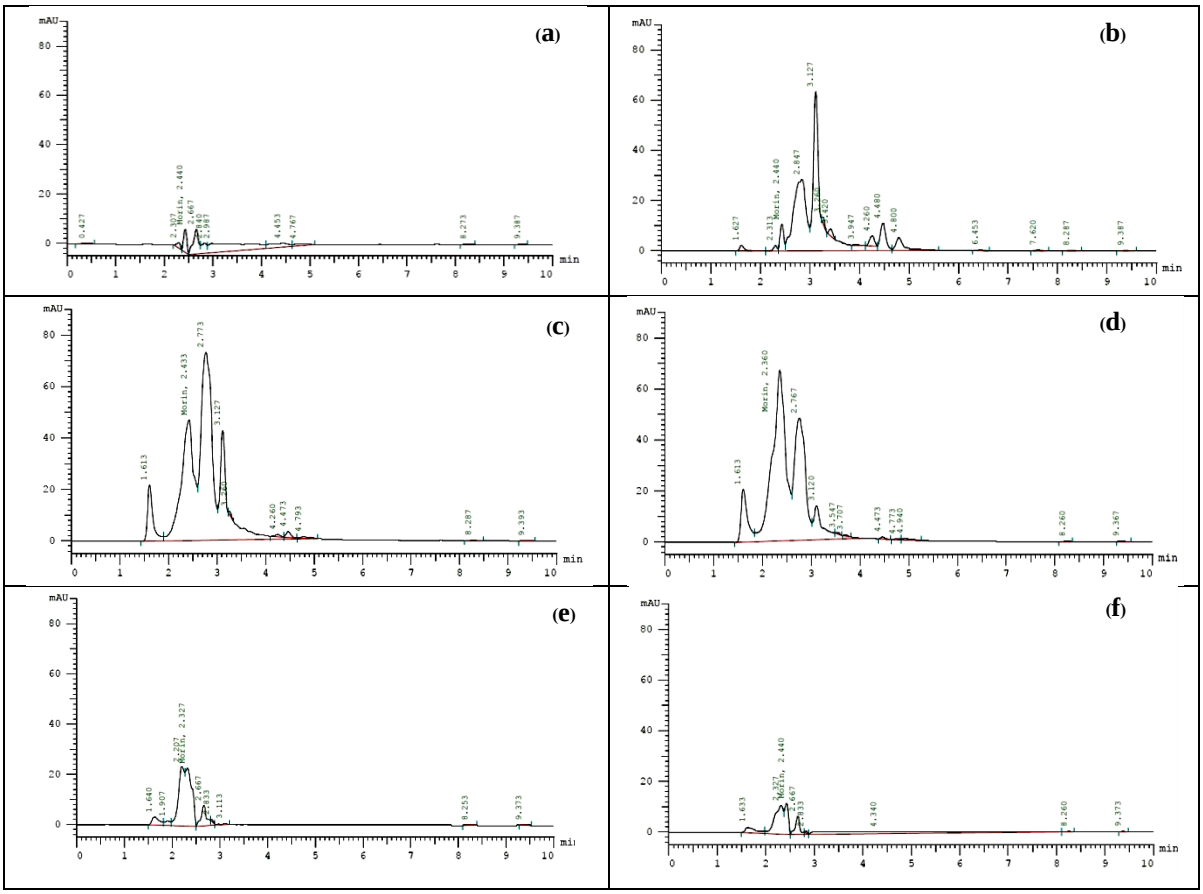

Figure 8. HPLC chromatograms of *M. alba* (CM60) leaf extracts in different solvents (a) hexane, (b) benzene, (c) ethyl acetate, (d) acetone, (e) ethanol, and (f) water

The HPLC method was validated for the analysis of morin content in the different solvent extracts of CM60. The linear curve of standard was generated by using morin hydrate (Sigma-Aldrich, Germany) dissolved in mobile phase at the concentration range of 1.25-10.0 μg/mL. The good linearity was exhibited by the 4-point calibration curve performed in triplicate with correlation coefficients (R^2) within the range of 0.9996-0.9999, which indicated that the method was effective for the quantification of morin. The HPLC chromatogram of morin in each extract of CM60 is presented in Figure 9.

https://doi.org/10.14456/jsat.2020.2

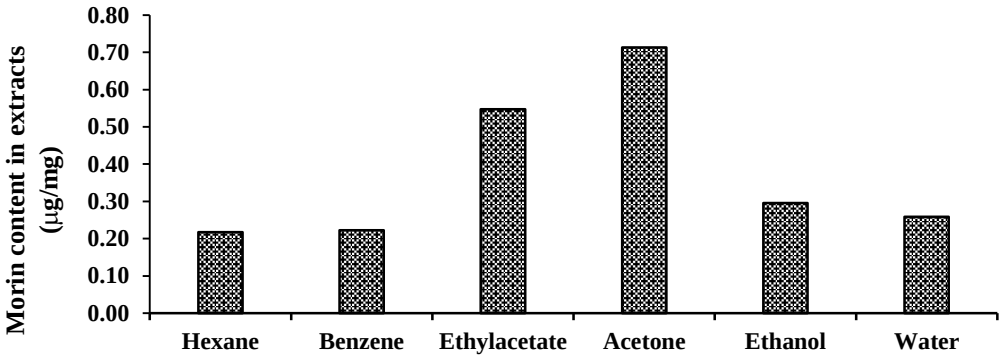

Figure 9. The morin content of *M. alba* (CM60) leaf extracts in different solvents.

The in-house validated HPLC method was applied to determine the contents of morin in the six different polar extracts of CM60. The results in Figure 9 showed that acetonic extract of CM60 possessed the greatest amount of morin, ranging in the order: that of ethyl acetate, ethanol, water, hexane = benzene. Interestingly, the acetonic extract of CM60 was revealed the greatest inhibitory effect of tyrosinase and related to the highest contents of flavonoid and morin. Therefore, it can be assumed that morin possessed inhibitory effect of tyrosinase accompany with other flavonoids such as rutin, maclurin, resveratrol, isoquercitrin and the others in the category of flavonols as the reports of Chang et al. (2011) and Yang et al. (2017).

Conclusions

The ethyl acetate extract of CM60 showed the greatest antioxidant inhibitory activity evaluated by using ABTS and DPPH assays and showed positively related to TPC content. Meanwhile, the acetonic extract from CM60 exhibited better tyrosinase inhibitory activity than other varieties and revealed positively related to the flavonoid content. Additionally, morin had a high content in the mulberry leaf extract from CM60 especially in acetonic extract, thus CM60 leaf extracted using acetone and ethyl acetate was the most suitable as potential resources for skin-whitening agent development.

Acknowledgements

The authors would like to thank the National Research Council of Thailand (Project no. 622993) and Rajamangala University of Technology Lanna, Thailand for their financial support and special thanks to Queen Sirikit Sericulture Center Chiang Mai for material support towards this project.

References

Abarca-Vargas, R., Peña Malacara, C.F. and Petricevich, V.L. 2016. Characterization of chemical compounds with antioxidant and cytotoxic activities in *Bougainvillea x buttiana* Holttum and Standl, (var. Rose) extracts. Antioxidants. 5(4). doi:10.3390/antiox5040045.

Agorku, E.S., Kwaansa-Ansah, E.E., Voegborlo, R.B., Amegbletor, P., and Opoku, F. 2016. Mercury and hydroquinone content of skin toning creams and cosmoetic soaps, and the potential risks to the health of Ghanaian women. SpringerPlus. 5: 319. doi: 10.1186/s40064-016-1967-1. eCollection 2016.

Andallu, B., Shankaran, M., Ullagaddi, R., and Iyer, S. 2014. *In vitro* free radical scavenging and *in vivo* antioxidant potential of mulberry (*Morus indica* L.) leaves. Journal of Herbal Medicine. 4(1): 10-17.

Andarwulan, N., Batari, R., Sandrasari, D.A., Bolling, B., and Wijaya, H. 2010. Flavonoid content and antioxidant activity of vegetables from Indonesia. Food Chemistry. 121(4): 1231–1235.

Aryal, S., Baniya, M.K., Danekhu, K., Kunwar, P., Gurung, R., and Koirala, N. 2019. Total phenolic content, flavonoid content and antioxidant potential of wild vegetables from western Nepal. Plants (Basel). 8(4): doi:10.3390/plants8040096.

Bae, S.H., and Suh, H.J. 2007. Antioxidant activities of five different mulberry cultivars in Korea. LWT- Food Science and Technology. 40(6): 955-962.

Chang, L-W., Juang, L-J., Wang, B-S., Wang, M-Y., Tai, H-M., Hung, W-J., Chen, Y-J., and Huang, M-H., 2011. Antioxidant and antityrosinase activity of mulberry (*Morus alba* L.) twigs and root bark. Food and Chemical Technology. 49: 785-790.

Chang, Y.C., Yang, M.Y., Chen, S.C., Wang, C.J. 2016. Mulberry leaf polyphenol extract improves obesity by inducing adipocyte apoptosis and inhibiting preadipocyte differentiation and hepatic lipogenesis. Journal of Functional Foods. 21: 249-262.

Chauhan, S., Verma, S. C., and Kumar, V. 2013. Evaluation of phytochemical and anti-oxidant activity in different mulberry varieties. Asian Journal of Chemistry. 25(14): 8010-8014.

Chon, S.U., Kim, Y.M., Park, Y.J., Heo, B.G., Park, Y.S., and Gorinstein, S. 2009. Antioxidant and antiproliferative effects of methanol extracts from raw and fermented parts of mulberry plant (*Morus alba* L.). European Food Research and Technology. 230: 231-237.

Cui, H., Lu, T., Wang, M., Zou, X., Zhang, Y., Yang, X., Dong, Y., and Zhou, H. 2019. Flavonoids from *Morus alba* L. leaves: Optimization of extraction by response surface methodology and comprehensive evaluation of their antioxidant, antimicrobial, and inhibition of α-amylase activities through analytical hierarchy process. Molecules. 24: 2398. doi:10.3390/molecules 24132398.

Hao, J.Y., Wan, Y., Yao, X.H., Zhao, W.G., Hu, R.Z., Chen, C., Li, L., Zhang, D.Y., and Wu, G.H. 2018. Effect of different planting areas on the chemical compositions and hypoglycemic and antioxidant activities of mulberry leaf extracts in Southern China. PLoS One. 13(6): e0198072. doi: 10.1371/journal.pone.0198072.

Hashemi, S., and Khadivi, A. 2020. Morphological and pomological characteristics of white mulberry (*Morus alba* L.) accessions. Scientia Horticulturae. 259: 108827. https://doi.org/10.1016/j.scienta.2019.108827

Hussain, F., Rana, Z., Shafique, H., Malik, A., and Hussain, Z. 2017. Phytopharmacological potential of different species of *Morus alba* and their bioactive phytochemicals: A review. Asian Pacific Journal of Tropical Biomedicine. 7(10): 950-956.

Kim, H.B. 2017. Comparison with various mulberry leaves' and fruit's extract in lipid accumulation inhibitory effect at adipocyte model. International Journal of Industrial Entomology. 35: 1-6.

Kim, I., and Lee, J. 2017. Comparison of different extraction solvents and sonication times for characterization of antioxidant activity and polyphenol composition in mulberry (*Morus alba* L.) Applied Biological Chemistry. 60: 509-517.

Li, H., Zhang, D., Tan, L-H., Yu, B., Zhao, S-P., and Cao, W-G. 2017. Comparison of the antioxidant properties of various solvent extracts from *Dipsacus asperoides* and identification of phenolic compounds by LC-ESI-QTOF-MS–MS. South African Journal of Botany. 109:1-8.

McGregor, D. 2007. Hydroquinone: An evaluation of the human risks from its carcinogenic and mutagenic properties. Critical Reviews in Toxicology. 33(10): 887-914.

Momtaz, S., Mapunya, B.M., Houghton, P.J., Edgerly, C., Hussein, A., Naidoo, S., and Lall, N. 2008. Tyrosinase inhibition by extracts and constituents of *Sideroxylon inerme* L. stem bark, used in South Africa for skin lightening. Journal of Ethnopharmacology.119(3):507-12. doi: 10.1016/j.jep.2008.06.006. Epub 2008 Jun 13.

Nasti, T. H. and Timares, L. 2014. Invited Review MC1R, Eumelanin and Pheomelanin: their role in determining the susceptibility to skin cancer. Photochemistry and Photobiology. 91(1): 188-200

Parvez, S., Kang, M., Chung, H.S., Cho, C., Hong, M.C., Shin, M.K., and Bae, H. 2006. Survey and mechanism of skin depigmenting and lightening agents. Phytotherapy Research. 20(11): 921-34.

Ranjan, B., Kumar, R., Verma, N., Mittal, S., Pakrasi, P.L., and Kumar, R.V. 2017. Evaluation of the antidiabetic properties of S-1708 mulberry variety. Pharmacognosy Magazine. 13: 280-288

Reichardt, C. 2003. Solvents and Solvent Effects in Organic Chemistry, 3rd ed., Wiley-VCH Verlag, Weinheim, Germany.

Riche, D.M., Riche, K.D., East, H.E., Barrett, E.K., and May, W.L. 2017.Impact of mulberry leaf extract on type 2 diabetes (Mul-DM): A randomized, placebo-controlled pilot study. Complementary Therapies in Medicine. 32: 105–108.

Ribeiro, A. S., Estanqueiro, M., Oliveira, M. B., and Lobo, J. M. S. 2015. Main Benefits and Applicability of Plant Extracts in Skin Care Products. Cosmetics. 2, 48-65.

Saravanakumar, K., Sarikurkcu, C., and Sarikurkcu, R.T. 2019. A comparative study on the phenolic composition, antioxidant and enzyme inhibition activities of two endemic *Onosma* species. Industrial Crops and Products. 142: 111878.

Sassa-deepaeng, T., Khamphira, T., Yodthong, W., and Wanapichit, V. 2017. Antibacterial antioxidant composition of *Eclipta prostrata*. Proceeding of 4th Conference on Research and Creative Innovations and 2nd International symposium on Application of High-voltage, Plasma and Micro/Nano Bubble to Agriculture and Aquaculture. 26-27 Jul 2017. Chiangmai Grandview Hotel and Convention Center, Chiang Mai, Thailand. p.664-671.

Sassa-deepaeng, T., Yodthong, W., and Khamphira, T. 2019. Green synthesized copper nanoparticles and their anti-bacterial properties against bullfrog multidrug resistant gram negative bacteria. Veterinary Integrative Sciences. 17(1): 33-49.

Sheng, Y., Zheng, S., Zhang, C., Zhao, C., He, X., Xu. W., and Huang, K. 2018. Mulberry leaf tea alleviates diabetic nephropathy by inhibiting PKC signaling and modulating intestinal flora. Journal of Functional Foods. 46: 118-127.

Solano, F. 2014. Melanins: Skin Pigments and Much More—Types, Structural Models, Biological Functions, and Formation Routes. New Journal of Science. Article ID 498276, doi.org/10.1155/2014/498276. Epub.

Sun, F., Shen, L., and Ma Z. 2011. Screening for Ligans of human aromatase from mulberry (*Mori alba* L.) leaf by using high-performance liquid chromatography/tandem mass spectrometry. Food Chemistry. 126: 1337-1343.

Thavamoney, N., Sivanadian, L., Tee, L.H., Khoo, H.E., Prasad, K.N., and Kong, K.W. 2018. Extraction and recovery of phytochemical components and antioxidative properties in fruit parts of *Dacryodes rostrata* influenced by different solvents. Journal of Food Science and Technology. 55(7): 2523-2532.

Ulbing C. K. S., Muuse, J.M., Miner, B.E. 2019 Melanism protects alpine zooplankton from DNA damage caused by ultraviolet radiation. Proceedings of the Royal Society B: Biological Sciences. 286: 20192075. http://dx.doi.org/10.1098/rspb.2019.2075 Epub.

https://doi.org/10.14456/jsat.2020.2

Ya, W., Chun-Meng, Z., Tao, G., Yi-Lin, Z., and Ping, Z. 2015. Preliminary screening of 44 plant extracts for anti-tyrosinase and antioxidant activities. Pakistan Journal of Pharmaceutical Sciences. 28(5): 1737-1744.

Yadav, A.V., and Nade, V.S. 2008. Anti-dopaminergic effect of the methanolic extract of *Morus alba* L. leaves. Indian Journal of Pharmacology. 40(5): 221-226.

Yang, J. Ou, X.Q., Zhang, X., Zhou, Z.Y., and Ma, L.Y., 2017. Effect of Different Solvents on the Measurement of phenolics and the antioxidant activity of mulberry (*Morus atropurpurea* Roxb.) with accelerated solvent extraction. Journal of Food Science. 82(3): 605-612. doi: 10.1111/1750-3841.13638. Epub.

Yun, H.Y., Kim, D.H., Son, S., Ullah, S., Kim, S.J., Kim, Y.J., Yoo, J.W., Jung, Y., Chun, P., and Moon, H.R. 2015. Design, synthesis, and anti-melanogenic effects of (E)-2-benzoyl-3-(substituted phenyl) acrylonitriles. Drug Design, Development and Therapy. 4(9): 4259-4268.

Zhang, H.W.; Chen, X.Y. and Ling, C.Y. 2010. Optimization of alcoholic extraction of flavonoids from mulberry leaves using response surface methodology. Amino Acids and Biotic Resources. 34: 76–79.

Zhang, L., Tao, G., Chen, J., and Zheng, Z-P. 2016. Characterization of a new flavone and tyrosinase inhibition constituents from the twigs of *Morus alba* L. Molecules. 21, 1130; doi:10.3390/molecules 21091130.

Zou, Y., Liao, S., Shen, W., Liu, F., Tang, C., Chen, C-Y.O., and Sun, Y. 2012. Phenolics and Antioxidant Activity of Mulberry Leaves Depend on Cultivar and Harvest Month in Southern China. International Journal of Molecular Sciences. 13(12): 16544–16553.

JSAT
Journal of Science and Agricultural Technology
Research Article
https://doi.org/10.14456/jsat.2020.3
e-ISSN 2730-1532, ISSN 2730-1524

Characteristics of yogurt supplemented with different concentrations of *Carissa carandas* L.

Ni-orn Chomsri[1]* and Kamonwan Manowan[2]

[1] Agricultural Technology Research Institute, Rajamangala University of Technology Lanna
[2] Faculty of Sciences and Agricultural Technology, Rajamangala University of Technology Lanna

***Corresponding author**: niornchomsri@rmutl.ac.th*
Received December 19, 2019. Revised February 9, 2020; March 22, 2020. Accepted March 22, 2020.

Abstract

Yogurt is a fermented dairy product claimed to confer health benefits due to the remaining viability of good lactic acid bacteria (LAB). This study investigates the influence of using *Carissa carandas* L. (CC) as a supplement in the yogurt. The yogurt samples were examined for their physicochemical, microbiological and sensory properties. Supplementation of CC berry in the yogurt improved the quality compared with 0% supplementation of CC berry. Yogurt with 20% CC berry exhibited the highest total phenolic compounds. LAB present in yogurt was remained above 8 log CFU/g after 21 day storage period at 4 ºC. Yogurt with CC berry supplements showed better sensory properties (moderately like to like very much) than yogurt without CC berry supplement ($p \leq 0.05$). The finding of this study suggests that CC berry is a potential plant-based component to improve both phytochemical and sensory properties in yogurt production.

Keywords: *Carissa carandas*, yogurt, lactic acid bacteria, phytochemicals

Introduction

Carissa carandas L. (CC) is an evergreen and spiny shrub belonging to Apocynaceae family (Weerawatanakorn and Pan, 2016), widely known in many local names, e.g. Carandas (Bansal, 2014), Karanda and Carunda (Kubola et al., 2011), Karaunda (Mehmood et al., 2014) Karamcha (Khatun et al., 2017). In Thailand, it is called Namdaeng (red thorn) or Manao Mai Ru Ho (Yuenyongphutthakal et al., 2012; Pewlong et al., 2014; Chomsri et al., 2018). The fruit turns from pinkish white to blackish purple when ripe and can be eaten raw or processed (Chomsri et al., 2018; Chomsri and Manowan, 2019). Mature fruit is useful for making jellies, jams, squash, syrup and chutney due to its high pectin content (Lapsongphon and Changso, 2019). The blackish purple fruit contains high composition of anthocyanin which is identified as cyanidin 3-rhamnoglucoside (Mohammad and Ding, 2019). The interest in CC has increased during the last decade especially studies on health effects because it is well recognized as an effective source of phytochemicals with excellent health benefits (Chomsri et al., 2017). Bhadane and Patil (2017) reported that the ripened CC berry was rich in flavonoids, e.g. rutin, epicatechin, quercetin and kaempferol including phenolics, e.g. syringic acid, vanillic acid and caffeic acid. Research on drying of CC berry pomace revealed its alternative use of the tablet product (Yuenyongphutthakal et al., 2012). Many reports claim pharmacological characteristics of CC such as treatment of constipation and diarrhea, stomachic, anorexia, intermittent fever, mouth ulcer and sore throat, syphilitic pain, burning sensation, scabies and epilepsy (Mehmood et al., 2014, Khatun et al., 2017; Bahdane and Pati, 2017).

Yogurt is a fermented dairy product, produced by the activity at 1:1 ratio of two well-known species of LAB, i.e. *Lactobacillus bulgaricus* and *Streptococcus thermophilus* converting lactose in milk to lactic acid and other flavor compounds under a controlled temperature and environmental conditions (Das et al., 2019). This results in a unique characteristics present in the finish product. The drop in pH caused by the production of lactic acid affects milk proteins to denature, providing yogurt with its characteristic texture and sour flavor (Hekmat and Reid, 2006). Nowadays, a strong focus on healthful, natural, and nutritional offerings on food influences millennial consumer behavior resulting in new development in food industry, including yogurt production. Various plant based components are combined into yogurt for consumer choice, which is generally associated with a healthier product (Sah et al., 2016; Barkallah et al., 2017; Tavakoli et al., 2018; Silva et al., 2019; Wang et al., 2020). In addition, sensory aspect has been considered very important to enhance consumption (Perina, 2015; Abdel-Hamid et al., 2020).

CC can exert several pharmacological effects because of their content of bioactive phytochemical compounds (Bhadane and Patil et al., 2017; Chomsri et al., 2017). Hence the aim of this

https://doi.org/10.14456/jsat.2020.3

study was to evaluate the performance of CC supplement in yogurt production. The influence of CC contents on physicochemical, microbiological and sensorial characteristics of produced yogurt was investigated.

Materials and methods

CC berry preparation

Fully ripe with blackish purple and sound CC was collected from Agricultural Technology Research Institute, Rajamangala University of Technology Lanna, Lampang, Thailand. After washing, sorting and deseeding, the CC flesh was mixed with sucrose at the ratio of 1:1 and heated at 90-95 ºC for 20 minutes.

Yogurt preparation

Yogurt samples were prepared by heating cow's milk at 90-95 ºC for 10 min and cooled down by 45 ºC. The milk was inoculated with commercial yogurt culture (Lyofast, Sacco Srl, Italy). The mixture of milk and starter yogurt culture was incubated at 45 ºC for 5 h or pH value was less than 4.5. Subsequently, CC berry contents at 4 levels based on yogurt (w/w), i.e. 0% (YCC0), 10% (YCC10), 15% (YCC15), and 20% (YCC20) were added and mixed with the plain yogurt. The CC yogurt samples were then packed in cups of 30 ml and stored at 4$\pm$1 °C before analysis at 0, 7, 14 and 21 days.

Microbiological enumeration

For the enumeration of viable cell counts, 10 g samples were collected directly after packing and storage for 24 h. The samples were serially diluted in 90 mL sterile Ringer's solution (NaCl 1.125 g/l, KCl 0.0525 g/l, $CaCl_2$ 0.03 g/l and $NaHCO_3$ 0.025 g/l). The diluted samples were plated on MRS (Merck, Darmstadt, Germany) and PCA (Merck, Darmstadt, Germany) for LAB and total bacterial count, respectively.

Chemical Analysis

pH was measured by digital pH meter (Model C831, Belgium) according to Nielsen (2017). Total acidity was determined by diluting each 5 ml aliquot of sample in 50 ml distilled water and then titrating to pH 8.2 using 0.1 N NaOH (Iland et al., 2000). Titratable acidity was expressed as citric acid and lactic acid percentages for CC berry and yogurt, respectively. Total soluble solid content was determined on an Atago hand-held refractometer. Free alpha amino nitrogen (FAN) was quantified by spectrophotometric method (Intaramoree and Chomsri, 2014) using the spectrophotometer (T80 UV, PG Instrments, England). Total anthocyanin content was evaluated by the pH-differential method of Giusti and Wrolstad (2005). The Folin-Ciocalte method was used to evaluate total phenolic content (Spínola et al., 2015). The antioxidant activity was determined by the ABTS method (Wongputtisin et al., 2007). The colorimetric protein assay was used to measure the concentration of total soluble protein (Bradford, 1976). Total sugar content was measured by phenol-sulfuric acid method (Nielsen, 2017).

Syneresis and water-holding capacity (WHC) evaluation

Syneresis defined as the formation of a liquid (whey) on top of the yogurt was measured using the centrifugation method according to Farnworth et al. (2006) with modification. 40 ml of yogurt was centrifuged at 500 x g for 10 min at 4 ºC. The clear supernatant was collected and weighed. The syneresis percentage was calculated as the percentage of separated whey from gel network during centrifuge. Water holding capacity (WHC) was measured as described by modified method of Serra et al. (2007) and Michael et al. (2010). 40 ml of yogurt was weighed and centrifuged at 5,000 *x g* at 10 ºC for 20 min. After centrifugation, separated supernatant was drained, whey was weighed using a sieve in order to ensure the absence of any curd particles. WHC was expressed as the percentage of grams of expelled whey per gram of yogurt. These measurements were performed in triplicate.

Sensory analysis

All the panelists were experienced in yogurt. A group of 30 panelists took part in this study. Yogurt products fermented for 5 h and stored for 24 h were evaluated for organoleptic quality. The samples of yogurt were served in random order at 4 °C in plastic cups identified with a random 3-digit code. The panelists were suggested to rinse their mouths with water between samples. Each panelist received 4 samples of yogurt to evaluate and comment on the sensory characteristics. The panelists were asked to evaluate the appearance, color, odor, flavor, texture and overall preference of the final product depending on a nine-point hedonic scale, ranging from 9 (like extremely liked) to 1 (extremely disliked) for each organoleptic characteristic (Meilgaard et al., 2006).

Statistical analysis

All the experiments were carried out with 3 replications. Analysis of variance (ANOVA) was used to compare mean differences of the samples. Significant differences between treatments were analyzed by Duncan's new multiple range test (DNMRT) at a 0.95 significance level. Values were expressed as the mean of all replicate determinations with standard deviation.

https://doi.org/10.14456/jsat.2020.3

Results and discussion

Composition of CC berry

The results showed that the pH and acidity of CC fruit were 3.11 and 1.71%, respectively, therefore, it could be classified in the group of high acid food (Potter, 1986). According to the total soluble solid (TSS) content of 10 ^{o}Brix, total sugar content of 72.79 mg/g and reducing sugar content of 63.36 mg/g containing in the CC berry, the low ratio of TSS/sugar and acid was obtained. This means that the CC fruit possessed the tangy and sour taste. Total phenolic content of 707.27 mg/kg and anthocyanin content of 112 mg/kg were found in the CC fruit in this study while Chomsri et al. (2017) reported higher contents of these phytochemical contents. This could probably be due to the cultivar and the ripening stage. Regarding to CC properties, addition of the fruit into yogurt could possibly serve as a source for functional foods.

Table 1. Properties of *Carissa carandas* L. fruit

Properties	Values
pH	3.11±1.23
Total acidity (% as citric acid)	1.71±0.04
Total soluble solids (^{o}Brix)	10±2.58
Free α-amino nitrogen (mg/kg)	228±11.48
Total phenolic content (mg/kg)	707±29
Total soluble protein content (mg/kg)	82.17±2.65
Antioxidant activity (% ABTS scavenging effect)†	35.36±1.67
Total sugar content (mg/g)	72.97±5.84
Reducing sugar content (mg/g)	63.36±10.52
Total anthocyanin content (mg/kg)	112±6

† Data obtained from 100-fold dilution of the sample

Physicochemical properties of yogurt

Different colors of the yogurt from four treatments were obviously seen (Figure 1). Intensity of pinkish red color was increased in yogurt samples supplemented with higher CC berry contents. The pinkish red color was associated with concentrations of red pigments of anthocyanins, e.g. cyanidin-3-O-glucoside, cyanidin-3-O-galactoside and delphinidin-3-O-galacto-side containing in CC fruit as described by Mohammad and Ding (2019). As observed in this study, the anthocyanin components were likely to solubilize and stable in the yogurt matrix which seemed to improve the attribute of color appearance in the yogurt.

a b c d

Figure 1. Yogurt supplemented with different CC berry contents; a) 0%, b) 10%, c) 15% and d) 20%

As shown in Table 2, the effect of CC supplements on pH values, titratable acidity and total solid contents were observed. Four yogurt treatments in this study reached essential quality of minimum titratable acidity of 0.6% expressed as lactic acid (Codex Alimentarius Commission, 2011). The yogurt product after fermentation had pH in the range of 3.43-3.91. The yogurt sample without CC berry supplement showed the highest pH value of 3.91 which was similar to previous reports of Bosnea et al. (2017) and Delgado-Fernandez et al. (2019). In contrast, yogurt samples with CC berry supplement had lower pH values. This reduction was likely due to acids containing in CC berry. Yogurt containing higher contents of CC berry displayed significantly higher titratable acidity and total soluble solids ($p \leq 0.05$). This probably caused by the added sugar during CC preparation and solid parts found in CC fruit such as organic acids, sugars, pigments and fibers (Sarkar et al., 2018; Mohammad and Ding, 2019). Acids found in the yogurt samples were possibly derived from two sources, i.e. fermentation

https://doi.org/10.14456/jsat.2020.3

of lactose to organic acids such as lactic acid and acetic acid (Delgado-Fernandez et al., 2019) and organic acids existing in CC berry as described above. The concentration of FAN in the yogurt samples of this study were between 68.35-72.49 mg/kg while milk was reported to have FAN in the amount of approximately 0.50 mg/kg based on the average molecular weight of an amino acid (Farvin et al., 2010; McPherson and Pincus, 2011). This could indicate the formation of free amino acids and peptides resulting from bacterial proteolysis during fermentation which is in accordance with previous findings (Serra et al., 2009; Farvin et al., 2010). Total soluble protein contents were dramatically decreased in yogurt supplemented with CC berry which was possibly caused by reduction of plain yogurt content and protein–phenolic interactions. (Rodtjer et al., 2019; Ozdal et al., 2013; Isik et al., 2014; Seczyk et al., 2019). This binding was stronger at low pH condition in yogurt leading to change in characteristics of protein and phenolic compounds as well as its functional properties.

Table 2. Chemical property of yogurt supplemented with different CC berry contents

Treatment	pH*	TA (%)*	TSS (ºBrix)*	FAN (mg/kg)ns	TSP (mg/kg)*
YCC0	3.91±0.04^{a}	0.72±0.02^{b}	6.00±0.00^{c}	72.49±0.71	3810±417^{a}
YCC10	3.71±0.02^{b}	0.80±0.04^{b}	17.00±0.00^{b}	69.26±2.71	200±10^{b}
YCC15	3.59±0.08^{b}	1.00±0.07^{a}	21.75±3.18^{b}	68.66±1.00	189±17^{b}
YCC20	3.43±0.02^{c}	1.07±0.02^{a}	27.00±1.41^{a}	68.35±1.43	165±24^{b}

ns denotes means are not significantly different (p>0.05)

* Means in a column with the different letters represent significant differences (p≤0.05)

Titratable acidity (% as lactic acid); TA, total soluble solids (°Brix); TSS, free alpha amino nitrogen (mg/kg); FAN, total soluble protein (mg/kg); TSP. Yogurt samples containing CC berry contents of 0% (YCC0), 10% (YCC10), 15% (YCC15) and 20% (YCC20).

Figure 2a shows the total sugar contents, syneresis and WHC in yogurt samples. Adding CC berry content of 20% led to the highest total sugar content compared with that of lower CC berry contents. It was obvious that sugar containing in the prepared CC berries was the main reason of the sugar increase. Syneresis, the whey separation from milk protein gel is considered as an important index of yogurt quality (Vareltzis et al., 2016). Yogurt sample without CC berry supplement was high susceptibility while syneresis amount was not observed in the samples with CC supplements (Figure 2b). Creation of a binding water through solids containing in CC supplements could be a reason of the syneresis improvement. A similar observation was reported by Akgün et al. (2020). In contrast, the yogurt with higher concentrations of carrot juice resulted in higher syneresis susceptibility (Kiros et al., 2016). It is worth noting that syneresis of CC yogurt in this experiment was lower 4 to 6 times compared to other plant based yogurt (Kiros et al., 2016; Akgün et al., 2020). Figure 2c illustrates WHC of the CC yogurt samples. It appeared that CC supplement likely lowered WHC in yogurt samples. WHC of CC yogurt in this study were in agreement with other plant based yogurt (Barkallah et al., 2017; Mousavi et al., 2019). Vareltzis et al. (2016) revealed that increasing total solids reduced pore size in the protein matrix of the yogurt gel which led to a reduction in syneresis and improvement of the water-holding capacity of the gel.

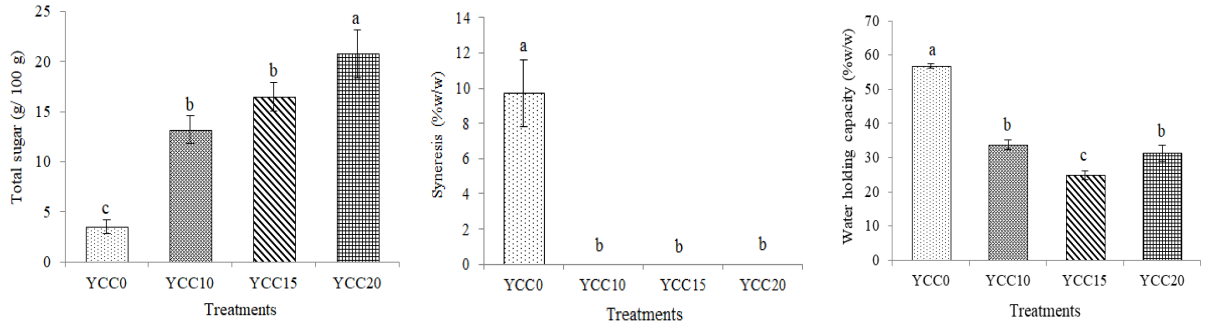

Figure 2. Total sugar contents (a), syneresis (b) and water holding capacity (c) of yogurt supplemented with different CC berry contents; YCC0, 0%; YCC10, 10%; YCC15, 15% and YCC20, 20%.

https://doi.org/10.14456/jsat.2020.3

Table 3 indicates the significant difference of phytochemical values in the yogurt samples. Yogurt supplemented with 20 % CC berry gave the best phytochemical profiles ($p \leq 0.05$) which was correlated with anthocyanin pigments and phenolic compounds containing in CC fruit (Pewlong et al., 2014; Weerawatanakorn and Pan, 2016; Chomsri et al., 2017; Sarkar et al., 2018). These substances were most typically responsible for the antioxidant activity exhibited in the CC yogurts. Previous reports showed variability of phytochemical values in yogurt which could possibly explained by many factors, e.g. types of plant, supplement amount, preparation during processing, analysis method. For examples, yogurt supplement with peppermint, carrot and green tea showed total phenolic compounds of 30 (Amirdivani and Baba, 2011), 36 (Kiros et al., 2016) and 3220 (Muniandy et al., 2016) mg GAE/ kg, respectively. It is interesting to note that yogurt samples with CC supplements produced remarkable antioxidant activity and total phenolic contents compared to other plants based yogurt (Kiros et al., 2016; Akgün et al., 2020; Pan et al., 2019).

Table 3. Phytochemical contents and antioxidant activity of CC berry yogurts

Treatment	AO (%)*	AOA (mg/100g)*	AOT (mg/100g)*	TPC (mg GAE/kg)*
YCC0	23.62 ± 0.43^{d}	6.43 ± 0.12^{d}	9.10 ± 0.16^{d}	106 ± 12^{c}
YCC10	61.86 ± 2.39^{c}	16.86 ± 0.65^{c}	23.84 ± 0.92^{c}	306 ± 7^{b}
YCC15	73.30 ± 1.26^{b}	19.98 ± 0.34^{b}	28.26 ± 0.49^{b}	323 ± 1^{b}
YCC20	95.29 ± 0.98^{a}	25.68 ± 0.26^{a}	36.73 ± 0.37^{a}	446 ± 45^{a}

* Means in a column with the different letters represent significant differences ($p \leq 0.05$)
Antioxidant activity (% scavenging effect); AO, ascorbic acid equivalent antioxidant capacity (mg/100g); AOA, trolox equivalent antioxidant capacity (mg/100g); AOT, total phenolic content (mg GAE/kg); TPC, yogurt supplemented with different CC berry contents; YCC0, 0%; YCC10, 10%; YCC15, 15% and YCC20, 20%.

Microbiological analysis

Total viable count and LAB count in yogurt samples are presented on Figure 3. Initial bacterial counts indicated LAB present in yogurt samples between 8.5-8.7 log CFU/g which typically meets recommendation of at least 6 log CFU/g at time of consumption (Codex Alimentarius Commission, 2011; Das et al., 2019). Furthermore, it was revealed that LAB survivability in yogurt samples stored at 4 ºC for 21 days was obviously remained stable. This finding supports existing of living LAB in CC yogurt which could probably provide health benefit regarding its potential properties of specific strains, e.g. probiotic property, producing bioactive metabolites (Das et al., 2019).

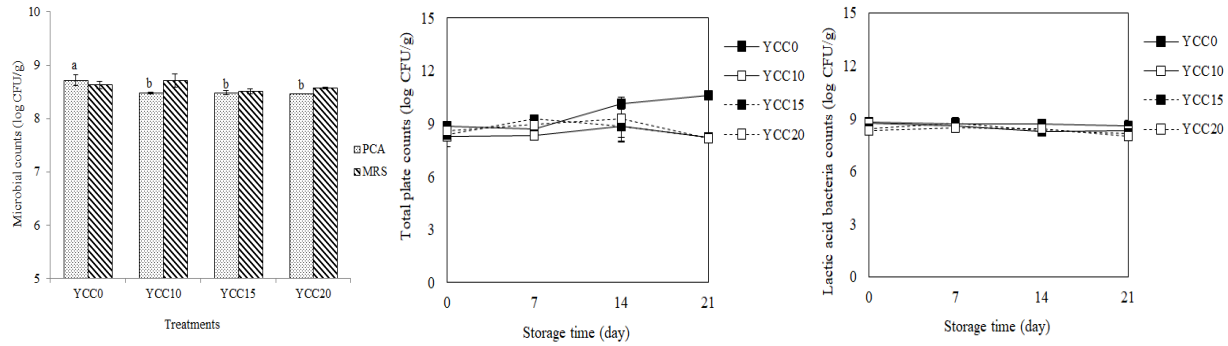

a b c

Figure 3. Initial total viable count and LAB count (a) in CC yogurt, changes of viable counts (b) and LAB counts (c) in yogurt supplemented with different CC berry contents; YCC0, 0%; YCC10, 10%; YCC15, 15% and YCC20, 20%.

Sensory analysis of yogurt

Sensory properties of yogurt, particularly flavor and texture/ mouthfeel are important for consumer acceptance (Das et al., 2019). In this study, addition of the prepared CC had significant effect of on the attributes of the sensory characteristic in yogurts. Yogurt with CC berry supplements displayed better sensory qualities ($p \leq 0.05$). Mean hedonic scores of odor, flavor and overall preference attributes were significantly higher in the yogurts containing CC berry reflecting the improved organoleptic properties, resulting from CC berry supplementation to the experimental yogurt. This might be explained by positive combination of CC berry and sugar containing in the prepared CC berry

https://doi.org/10.14456/jsat.2020.3

could enhance greater acceptability in the yogurt product. Based on sensory attributes presented in this study, the yogurt with 15% CC exhibited the best acceptance.

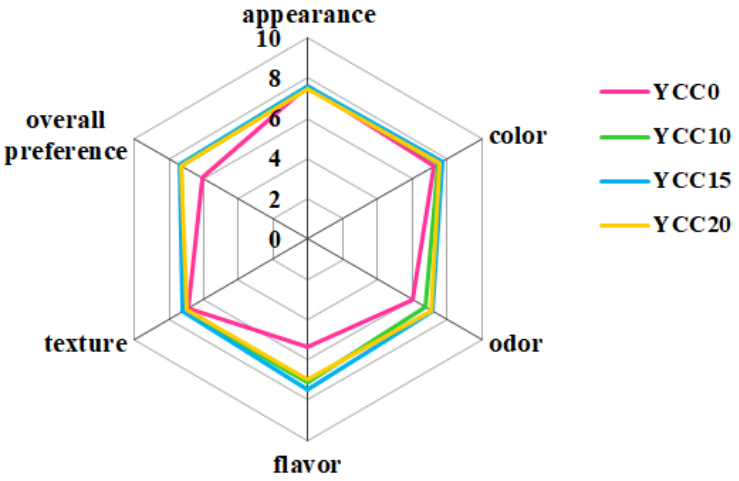

Figure 4. Effect of CC berry supplementation on sensory quality of yogurt supplemented with different CC berry contents; YCC0, 0%; YCC10, 10%; YCC15, 15% and YCC20, 20%.

Conclusion

In conclusion, CC berry supplementation in yogurt gave positive effects to yogurt product quality. Yogurt with 20% CC berry exhibited the highest phytochemical properties of phenolic compounds and antioxidant activity whereas yogurt with 15% CC berry showed the highest sensory properties. In addition, LAB survival throughout the storage period is a promising evidence to warrant further development of CC based product to obtain healthier yogurt.

References

Abdel-Hamida, M., Romeih, E., Huang, Z., Enomoto, T., Huang, L., and Li, L. 2020. Bioactive properties of probiotic set-yogurt supplemented with *Siraitia grosvenorii* fruit extract. Food Chemistry. 303: 125400.

Akgün, D., Gültekin-Ozgüven, M., Yücetepe, A., Altin, G., Gibis, M., Weiss, J., and Ozçelik, B. 2020. Stirred-type yoghurt incorporated with sour cherry extract in chitosan-coated liposomes. Food Hydrocolloids. 101: 105532.

Amirdivani, S., and Baba, A.S. 2011. Changes in yogurt fermentation characteristics, and antioxidant potential and *in vitro* inhibition of angiotensin-1 converting enzyme upon the inclusion of peppermint, dill and basil. LWT - Food Science and Technology. 44: 1458-1464.

Bansal, L. 2014. *Carissa carandas* as a natural colourant and its effect on physical and fastness properties of silk. An International Quarterly Journal of Biology & Life Sciences. 2(2): 470-474.

Barkallah, M., Dammak, M., Louati, I., Hentati, F., Hadrich, B., Mechichi, T., Ayadi, M.A., Fendri, I., Atti, H., and Abdelkafi, S. 2017. Effect of Spirulina platensis fortification on physicochemical, textural, antioxidant and sensory properties of yogurt during fermentation and storage. LWT - Food Science and Technology. 84: 323-330.

Bhadane, B.S., and Patil R.V. 2017. Isolation, purification and characterization of antioxidative steroid derivative from methanolic extract of *Carissa carandas* (L.) leaves. Biocatalysis and Agricultural Biotechnology. 10: 216-223.

Bosnea, L.A., Kopsahelis, N., Kokkali, V., Terpou, A., and Kanellaki, M. 2017. Production of a novel probiotic yogurt by incorporation of *L. casei* enriched fresh apple pieces, dried raisins and wheat grains. Food and Bioproducts Processing. 102: 62–71.

Bradford, M.M. 1976. A rapid and sensitive method for quantitation of microgram quantities of protein utilizing the principle of protein-dye-binding. Analytical Biochemistry. 72, 248-254.

Chomsri, N., Yangprasert, J., Wongkeaw, P., and Manowan, K. 2017. Morphological and physicochemical properties of Karanda (*Carissa carandas* L.) at the ripening stage based on different clones. In Proc. The 8th Rajamangala University of Technology International Conference (8th RMUTIC) "Creative RMUT and Sustainable Innovation for Thailand 4.0". IMPACT Muang Thong Thani Exhibition and Convention during 7-9 August 2017, Bangkok, Thailand. pp.135-141.

Chomsri, N., Yangprasert, J., Wongkeaw, P., and Manowan, K. 2018. Effects of carbon sources and inoculation protocols on carissa acetification process. Proceeding: The 8th Rajamangala University of Technology International Conference (9th RMUTIC) "RMUT driving innovation for Thailand 4.0". Rau Rasada Hotel, during 1th-3rd August 2017, Trang, Thailand. pp.2 20-230.

Chomsri, N., and Manowan, K. 2019. Effect of Inulin and *Carissa carandas* L. supplementation on physicochemical and microbiological properties of frozen yogurt. CIGR VI 2019 International Joint Conference on JSAM and SASJ, and CIGR VI Technical Symposium joining FWFNWG and FSWG Workshops" 3-6 September 2019, Hokkaido University. Sapporo, Japan.

Codex Alimentarius Commission. 2011. Milk and milk products. World Health Organization and Food and Agriculture Organization of The United Nations. Rome, 244 p.

Das, K., Choudhary, R., and Thompson-Witrick, K.A. 2019. Effects of new technology on the current manufacturing process of yogurt-to increase the overall marketability of yogurt. LWT - Food Science and Technology. 108: 69–80.

https://doi.org/10.14456/jsat.2020.3

Delgado-Fernandez, P., Corzo, N., Olano, A., Hernandez-Hernandez, O., and Moreno, F.J. 2019. Effect of selected prebiotics on the growth of lactic acid bacteria and physicochemical properties of yoghurts. International Dairy Journal. 89: 77-85.

Farnsworth, J.P., Hendricks, L.G.M., and Guo, M.R. 2006. Effects of transglutaminase treatment on functional properties and probiotic culture survivability of goat milk yogurt. Small Ruminant Research. 65: 113–121.

Farvin, K.H.S., Baron, C.P., Nielsen, N.S., Otte, J., and Jacobsen, C. 2010. Antioxidant activity of yoghurt peptides: Part 2 – Characterisation of peptide fractions. Food Chemistry. 123(4): 1090-1097.

Giusti. M.M., and Wrolstad, R.E. 2005. Characterization and Measurement of Anthocyanins by UV-Visible Spectroscopy, pp. 19-31, In: Wrolstad, R.E., ed. Handbook of Food Analytical Chemistry (Vol 2): Pigment, Flavors, Texture and Bioactive Food Components. John Wiley and Sons. Inc., New Jersey.

Hekmat, S., and Reid, G. 2006. Sensory properties of probiotic yogurt is comparable to standard yogurt. Nutrition Research Reviews. 26: 163–166.

Iland, P., Ewart, A., Markides, A., Sitters, J., and Bruer, N. 2000. Techniques for chemical analysis and quality monitoring during winemaking. Patrick Iland Wine Promotions, Adelaide.

Işık, N., Alteheld, B., Kühn, S., Schulze-Kaysers, N., Kunz, B., Wollseifen, H.R., Stehle, P., and Lesser, S. 2014. Polyphenol release from protein and polysaccharide embedded plant extracts during in vitro digestion. Food Research International 65: 109–114.

Intaramoree, S., and N. Chomsri. 2014. Miso produced from different Thai rice cultivars: physicochemical and sensory characteristics. pp. 487-495. In K. Boonlertnirun, ed., The 5th Rajamangala University of Technology International Conference: The Technology and Innovation toward ASEAN. Rajamangala University of Technology Suvarnabhumi, Phranakhon Si Ayutthaya, Thailand.

Khatun, M., Habib, M.R., Rabbi, M.A., Amin, R., Islam, M.F., Nurujjaman, M., Karim, M.R., and Rahman, M.H. 2017. Antioxidant, cytotoxic and antineoplastic effects of Carissa carandas Linn. Leaves. Experimental and Toxicologic Pathology. 69(7): 469-476.

Kiros, E., Seifu, E., Bultosa, G., and Solomon, W.K. 2016. Effect of carrot juice and stabilizer on the physicochemical and microbiological properties of yoghurt. LWT - Food Science and Technology 69: 191-196.

Kubola, J., Siriamornpun, S., and Meeso, M. 2011. Phytochemicals, vitamin C and sugar content of Thai wild fruits. Food Chemistry. 126: 972–981.

Lapsongphon, N., and Changso, S. 2019. Development of reduced calories *carissa carandas* sherbet by substitution sugar with stevia extract. Food and Applied Bioscience Journal. 7(Special Issue on Agriculture and Agro-Industry): 162–171.

McPherson, R.A. and Pincus, M.R. 2011. Henry's Clinical Diagnosis and Management by Laboratory Methods. Elsevier Health Sciences, St. Louis. 1568 p.

Mehmood, M.H., Anila, N., Begum, S., Syed, S.A., Siddiqui, B.S., and Gilani, A.H. 2014. Pharmacological basis for the medicinal use of *Carissa carandas* in constipation and diarrhea. Journal of Ethnopharmacology. 153: 359-367.

Meilgaard, H., Civille, G.V., and Carr, B.T. 2006. Sensory evaluation techniques. CRC Press. Boca Raton.

Michael, M., Phebus, R.K., and Schmidt, K.A. 2010. Impact of a plant extract on the viability of *Lactobacillus delbrueckii* ssp. *Bulgaricus* and *Streptococcus thermophilus* in nonfat yogurt. International Dairy Journal. 20: 665-672.

Mohammad, M., and Ding, P. 2019. Physico-textural and cellular structure changes of *Carissa congesta* fruit during growth and development. Scientia Horticulturae. 246: 380–389.

Mousavi, M., Heshmati, A., Garmakhany, A.D., Vahidinia, A., and Taheri, M. 2019. Optimization of the viability of Lactobacillus acidophilus and physicochemical, textural and sensorial characteristics of flaxseed-enriched stirred probiotic yogurt by using response surface methodology. LWT - Food Science and Technology. 102: 80–88.

Muniandy, P., Shori, A.B., and Baba, A.S. 2016. Influence of green, white and black tea addition on the antioxidant activity of probiotic yogurt during refrigerated storage. Food Packaging and Shelf Life. 8: 1–8.

Nielsen, S.S. 2017. Food Analysis Laboratory Manual. Springer. Lafayette, Indiana. 249 p.

Ozdal, T., Capanoglu, E., and Altay, F. 2013. A review on protein–phenolic interactions and associated changes. Food Research International. 51: 954–970.

Pan, L., Liu, F., Luo, S., and Luo, J. 2019. Pomegranate juice powder as sugar replacer enhanced quality and function of set yogurts: Structure, rheological property, antioxidant activity and in vitro bioaccessibility. LWT - Food Science and Technology. 115: 108479.

Perina, N.P., Granato, D., Hirota, C., Cruz, A.G., Bogsan, C.S.B., and Oliveir, M.N. 2015. Effect of vegetal-oil emulsion and passion fruit peel-powder on sensory acceptance of functional yogurt. Food Research International. 70: 134–141.

Pewlong, W., Sajjabut, S., Eamsiri, J., and Chookaew, S. 2014. Evaluation of antioxidant activities, anthocyanins, total phenolic content, vitamin C content and cytotoxicity of *Carissa carandas* Linn. CMUJNS Special Issue on Food and Applied Bioscience. 13(1): 509–517.

Potter, N. 1986. Food Science. Springer. Netherlands. 735 p.

Rødtjer, A., Skibsted, L.H., and Andersen, M.L. 2010. The role of phenolic compounds during formation of turbidity in an aromatic bitter. Food Chemistry 123: 1035–1039.

Sarkar, R., Kundu, A., Banerjee, K., and Saha, S., 2018. Anthocyanin composition and potential bioactivity of karonda (*Carissa carandas* L.) fruit: An Indian source of biocolorant. LWT - Food Science and Technology. 93: 673-678.

Sah, B.N.P., Vasiljevic, T., McKechnie, S., and Donkor, O.N. 2016. Physicochemical, textural and rheological properties of probiotic yogurt fortified with fiber-rich pineapple peel powder during refrigerated storage. LWT - Food Science and Technology. 65: 978-986.

Seczyk, L., Swieca, M., Kapusta, I., and Gawlik-Dziki, U. 2019. Protein–phenolic interactions as a factor affecting the physicochemical properties of white bean proteins. Molecules. 24: 408.

Serra, M., Trujillo, A.J., Quevedo, J.M., Guamis, B., and Ferragut, V. 2007. Acid coagulation properties and suitability for yogurt production of cows' milk treated by high-pressure homogenization. International Dairy Journal. 17: 782–790.

Serra, M., Trujillo, A.J., Guamis, B., and Ferragut, V. 2009. Proteolysis of yogurts made from ultra-high-pressure homogenized milk during cold storage. Journal of Dairy Science. 92(1): 71-78.

Silva, S.C., Fernandes, I.P., Barros, L., Fernandes, A., Alves, M.J., Calhelha, R.C., Pereira, C., Barreira, J.C.M., Manrique, Y., Collac, E., Ferreira, I.C.F.R., and Barreiro, M.F. 2019. Spray-dried *Spirulina platensis* as an effective ingredient to improve yogurt formulations: Testing different encapsulating solutions. Journal of Functional Foods. 60: 103427.

https://doi.org/10.14456/jsat.2020.3

Spínola, V., Pinto, J., and Castilho, P.C. 2015. Identification and quantification of phenolic compounds of selected fruits from Madeira Island by HPLC-DAD–ESI-MSn and screening for their antioxidant activity. Food Chemistry. 173: 14-30.

Tavakoli, H., Hosseini, O., Jafari, S.M. and Katouzian, I. 2018. Evaluation of physicochemical and antioxidant properties of yogurt enriched by olive leaf phenolics within nanoliposomes. Journal of Agricultural and Food Chemistry 66: 9231−9240.

Vareltzis, P., Adamopoulos, K., Stavrakakis, E., Stefanakis, A., and Goula, A.M. 2016. Approaches to minimise yoghurt syneresis in simulated tzatziki sauce preparation. International Journal of Dairy Technology. 69(2): 191-199.

Wang, X., Kristo, E., and LaPointe, G. 2020. Adding apple pomace as a functional ingredient in stirred-type yogurt and yogurt drinks. Food Hydrocolloids. 100: 105453.

Weerawatanakorn, M., and Pan, M. 2016. Phytochemical components of *Carissa carandas* and the inhibitory effects of fruit juice on inducible nitric oxide synthase and cyclooxygenase-2. Food Biochemistry. https://doi.org/10.1111/jfbc.12343.

Wongputtisin, P., Khanongnuch, C., Pongpiachan, P., and Lumyoung, S. 2007. Antioxidant activity improvement of soybean meal by microbial fermentation. Research Journal of Microbiology. 2(7): 577-583.

Yuenyongphutthakal, W., Khongsomphet, S., and Weeraphae, P. 2012. Drying of karanda berry (*Carissa carandas*) pomace and its tablet product. KKU Science Journal. 40(3): 877-889.

JSAT
Journal of Science and Agricultural Technology
Research Article
https://doi.org/10.14456/jsat.2020.4
e-ISSN 2730-1532, ISSN 2730-1524

Coconut and to a lesser extent krabok oil, depress rumen protozoa in beef cows

Paiwan Panyakaew[1]*, Jan Thomas Schonewille[2], Veerle Fievez[3], Gunjan Goel[4,5], Nico Boon[6], Chalermpon Yuangklang[7], Wouter Hendriks[2,8]

[1] Department of Animal Science, Faculty of Natural Resources, Rajamangala University of Technology Isan, Sakon-Nakhon Campus, Sakon Nakhon 47160 Thailand;
[2] Department of Farm Animal Health, Faculty of Veterinary Medicine, Utrecht University, Utrecht, The Netherlands;
[4] Laboratory for Animal Nutrition and Animal Product Quality (Lanupro), Faculty of Bioscience Engineering, Ghent University, Proefhoevestraat 10, 9090 Melle, Belgium;
[5] Department of Biotechnology and Bioinformatics, Jaypee University of Information Technology, Solan, India;
[6] Laboratory of Microbial Ecology and Technology (LabMET), Faculty of Bioscience Engineering, Ghent University, Gent, Belgium;
[7] Department of Agricultural Technology and Environment, Faculty of Science and Liberal Arts, Rajamangala University of Technology-Isan, Nakhon Ratchasima, 3000 Thailand
[8] Department of Animal Sciences, Wageningen University, Wageningen, The Netherlands;

***Corresponding author**: *paiwan_pyk@yahoo.com*
Received January 25, 2020. Revised March 3, 2020; March 12, 2020. Accepted March 22, 2020.

Abstract

Krabok and coconut oil were assessed for their ability to affect rumen protozoa via a 3×3 Latin square design with three rumen cannulated beef cows. The diets consisted of a TMR supplemented with either 25.5 g/kg of tallow (control) or the same quantity of coconut oil or krabok oil. The animals were fed restricted amounts (DM) of the experimental rations (1.5% of body weight per d) for 28 d per period. The samples of rumen fluid were collected on day 23 and 27 of each period, 0, 3, 6, 9 and 12h after morning feeding. Protozoa numbers decreased by 0.33 log units in the coconut ($P<0.05$) and 0.21 log units in the krabok oil diet ($P<0.05$) compared with the control diet. The ciliate value was not significantly different between treatment but were strongly ($R^2 = 0.88$) linearly associated with protozoa counts. The concentration of total VFA was not affected ($P = 0.804$) by the diet. Except propionic acid which showed a trend ($P = 0.056$), the proportions of the remaining VFA were not significantly ($P>0.10$) different between treatments. The propionate proportion was only reduced by supplementation of coconut oil to the TMR. Neither oils affected amylolytic, cellulolytic or proteolytic bacteria counts. Cluster analysis of the DGGE profile showed two clusters of ciliate communities, one including all the T diet-fed animals. All except one DGGE profile of a cow fed the KO diet group into the second cluster. Coconut oil, and to a lesser extent krabok oil, has a marked effect on the numbers of rumen protozoa.

Keywords: krabok oil, coconut oil, rumen protozoa, ciliate

Introduction

Methane produced during anaerobic fermentation in the rumen represents 2 to 12% gross energy loss to the host animal and contributes 15-20% to the global production of methane (Lila et al., 2003; Asanuma et al., 1999). Methane is produced by Archaea and they exist both as free-living organisms and in a symbiotic relationship with rumen protozoa (Finlay et al., 1994). The latter explains, at least partly, why defaunation of the rumen content is beneficial to mitigate methane emission (Hook et al., 2010). The defaunating effect of lipids depends on its fatty acid composition with medium chain fatty acids being more effective than polyunsaturated fatty acids in controlling the protozoal numbers (Guyader et al., 2014).

Krabok oil is derived from krabok seeds (*Irvingia malayana* Oliv. ex w.Benn) and contains roughly equal amounts of C12:0 and C14:0, i.e. 45% of total fatty acids (Wongsuthavas et al., 2007; Panyakaew et al., 2013a). Previously, Panyakaew et al. (2013a) have shown that, under *in vitro* conditions, krabok oil reduced the production of methane. The mode of action of krabok oil on methanogenesis was, however, not clear (Panyakaew et al., 2013a). In a subsequent *in vivo* study, Panyakaew et al. (2013b) demonstrated that krabok oil *versus* tallow reduced the log copy numbers of protozoa by 32.2%. This result can be interpreted in that the krabok oil reduced methanogenesis attributed, at least partly, to its antiprotozoal effect. Currently, the study of Panyakaew et al. (2013b) is the only study reporting on the defaunating action of krabok oil under *in vivo* conditions and thus

https://doi.org/10.14456/jsat.2020.4

the aforementioned result needs confirmation. Therefore, in the current study we focus on the potential of krabok oil to reduce the numbers of the ciliate protozoa. Coconut oil, which is particularly rich in lauric (C12:0) and, to a lesser extent, myristic (C14:0) acid, was used as a positive control because it is well known for its methane-suppressing activity (Dohme et al., 1999, Jordan et al., 2006, Machmüller and Kreuzer, 1999, Panyakaew et al., 2013b).

Materials and methods

Animals and experimental design

Three beef cows (Brahman x Thai native crossbreds) average body weight 429 ± 43 kg with permanent indwelling rumen cannulas were used in a 3×3 Latin square design study which was preceded by a 14-d pre-experimental adaptation period. The animals were housed under natural environmental conditions in individual pens (2×4 m^2) with 50% of the floor covered by concrete and the other half by sand. The study was conducted at department of Animal Science, Faculty of Natural Resources, Rajamangala University of technology Isan, Sakon-Nakhon campus. Sakon Nakhon, in the northeast and plateau region of Thailand. Approximately 172 meters above sea level. During this period, the cows were fed a basal ration as a total mixed ration (TMR) consisting of (g/kg TMR): cassava chips, 421.0; rice straw 210.5; dry tomato pomace, 157.9; molasses, 73.7; rice bran, 52.6; soya bean meal, 31.6; urea, 21.0; salt, 10.5; di-calcium phosphate, 7.4; oyster meal, 5.3; mineral premix, 5.3; and sulfur, 3.2. Each experimental period lasted 28 d with cows randomly assigned to each sequence of feeding on the three experimental rations (Table 1). Animals had *ad-libitum* access to water during the pre- and experimental periods and body weights were measured at the beginning of each experiment period.

Table 1. Sequence of experimental treatments in a 3×3 Latin square design experiment with 3 treatments (supplementation (25 g/kg DM) with either beef tallow, coconut oil or krabok oil) and 3 fistulated beef cows (B) in each of the three periods, the amount of oil/fat added to each treatment and the supply of total medium chain fatty acids (C10:0+C12:0+C14:0).

Parameter	Tallow	Coconut oil	Krabok oil
Period			
1	B1	B2	B3
2	B2	B3	B1
3	B3	B1	B2
Fat/oil source (g/kg DM)			
Tallow	25	0	6.3
Coconut oil	0	25	0
Krabok oil	0	0	19.2
Fatty acids (g/kg DM)*			
C10:0	0.02 ± 0.00	1.10 ± 0.58	0.44 ± 0.13
C12:0	0.03 ± 0.01	11.0 ± 0.38	8.85 ± 0.70
C14:0	0.89 ± 0.08	4.61 ± 0.45	8.53 ± 0.50
Total C10:0+C12:0+C14:0	0.94 ± 0.07	16.7 ± 0.55	17.8 ± 0.36
C12:0 to C14:0 ratio	0.04 ± 0.01	2.40 ± 0.23	1.04 ± 0.14

*average ± standard deviation of four batches.

Experimental rations

The three isolipidic experimental rations were a TMR with either: (1) 25.5 g/kg DM tallow (T), (2) 25.5 g/kg DM coconut oil (CO), or (3) 19.2 g/kg DM krabok oil +6.3 g/kg DM tallow (KO). Treatment 3 was designed to provide similar amounts of MCFA compared to treatment CO (Table 1). Besides C12:0 and C14:0, C10:0 was also balanced between the experimental ration because the latter has been shown to effectively reduce methane production and/or the number of protozoa and methanogens (Dohme et al., 2001, Goel et al., 2009). Dietary inclusion of oil supplements in the KO treatment was based on fatty acid compositions of the oils used in the previous experiments of Panyakaew et al. (2013a,b). All the oils were from the same batch as the latter study but were stored in airtight containers for 3 months longer. The fatty acid composition of the oil/fat is provided in Table 2. The animals were fed restricted amounts (DM) of the experimental rations (1.5% of body weight) to ensure a constant intake of non-variable nutrients. The rations were offered daily in two equal portions at 07:30 and 16:00h, and feed refusals, if any, were recorded.

https://doi.org/10.14456/jsat.2020.4

Table 2. Fatty acid composition (g/100 g fatty acids) of the coconut oil, krabok oil, tallow and total mixed ration (TMR).

Fatty acid	Tallow	Coconut oil	Krabok oil	TMR
C8:0	0.01	0.21	0.00	0.00
C10:0	0.05	2.10	1.58	0.28
C12:0	0.12	45.8	42.0	0.12
C14:0	3.97	20.5	46.4	0.38
C16:0	26.8	11.1	4.49	15.7
C18:0	25.7	3.22	0.41	6.42
C18:1 c9	23.5	13.1	2.57	25.9
C18:1 c11	1.16	0.42	0.43	0.96
C18:2 n-6	0.53	2.63	0.32	42.2
C18:3 n-3	0.39	0.02	0.04	0.00
C18:2 c9t11	0.37	-	-	0.23

Rumen sample collection

Rumen contents (~200 ml) were collected on day 23 and 27 of each period at 0, 3, 6, 9 and 12h after the morning feeding by sampling in different directions of the rumen. After thorough mixing, the samples were divided into three portions: the first aliquot of ~10 ml was stored at -80 °C until DNA extraction; the second aliquot of ~10 ml was acidified with 0.2 ml phosphoric:formic (10:1) and stored at -20 °C until analysis of volatile fatty acids (VFA). The third aliquot of ~1 ml was fixed with 10% formalin saline solution (37% to 40% formalin in 0.9% (w/v) normal saline solution, 1:9) and stored at 4 °C for microscopical protozoa counting. For the VFA analysis, acidified rumen fluid samples were mixed per day (0, 3, 6, 9 and 12h) per cow. Rumen fluid samples from day 27 were pooled per cow before DNA extraction. Individual rumen fluid samples were used for protozoa and bacteria counts.

Volatile fatty acids

Samples for the analysis of VFA were pooled within a day per cow, and then centrifuged at 15,000×*g* (4 °C) for 10 min. Thereafter, the supernatant was filtered through a nylon membrane (0.2 µm) and transferred into vials. The VFA was analyzed by gas chromatography (Schimadzu GC-14A, Belgium) as described by Van Ranst et al. (2010).

Microbiota counts

Total protozoa were counted using a haemacytometer (Boeco, hamburg, Germany) of 0.1 mm depth and a microscope (Model Olympus BX50). Twenty aliquots per sample were counted (Galyean, 1989). The media of Hobson (1969) were used to determine amylolytic, cellulolytic and proteolytic bacteria groups using the roll tube method (Hungate, 1969)

Quantitative polymerase chain reaction (qPCR)

Ciliate protozoa and total bacterial rRNA gene copies present in DNA extract of each ruminal digesta sample were quantified as described by Boeckaert et al. (2008) and Boon et al. (2003). The QIAamp Stool Kit was used to extract total DNA from a 0.4 g rumen sample following the protocol for 'Isolation of DNA from the stool for Pathogen Detection' in the handbook supplied by Qiagen Ltd. (Crawley, UK), according to the manufacturer's recommendation. *Butyrivibrio* rRNA gene copies present in DNA extract of each sample were quantified using an ABI Prism SDS 7000 instrument (Applied Biosystems, Lennik, Belgium) following the principle of Boeckaert et al. (2007). Dilutions (1:20) of DNA from all samples were added to amplification reactions (25 µl) containing 12.5 µl SYBR Green PCR Master Mix (Applied Biosystems, Warrington, UK), 6 µl RNA free water, 0.75 µl B395f primer (10 µM stock), 0.75 µl B812r primer (10 µM stock) and 5 µl DNA. Cycling conditions were 1 cycle of 50 °C for 2 min and 95 °C for 10 min and 40 cycles of 95 °C for 1 min; 54 °C for 30 s and 60 °C for 1 min. Measurements were done in triplicate for each run. A standard curve for qPCR was constructed using six different DNA concentrations (n=3), ranging from 2.67 copies to 2.67 × 108 copies of DNA per µl. A *Butyrivibrio* 417 bp PCR fragment inserted in a TOPO vector was used as a template for the standard curve. The slope of the standard curve was -3.42 (R^2=0.99).

Diversity of ciliate protozoa

Total DNA was extracted from 0.5 g of rumen sample following the method of Boeckaert et al. (2007). A nested PCR approach was used to amplify a fragment of the 18S rRNA gene of ciliates for DGGE (Boeckaert et al., 2007). In the first PCR, the general eukaryotic primer Euk1A and the ciliate specific primer 539r were combined. In the second PCR run, the ciliate specific primer 316f and the general eukaryotic primer Euk516r-GC were used (applied from Yu and Morrison, 2004). By using this specific combination of primers, most of the degeneracies present in the ciliate specific primers

https://doi.org/10.14456/jsat.2020.4

were avoided for DGGE analysis. The final concentrations of the different components in the Master Mix were according to the manufacturer's instructions (Promega, Madison, USA) and contained 1 µl DNA extract (first run) or 1 µl of PCR product (second run), 1 µl of each primer (10 µM stock), 1 µl dNTP mix (0.2 mM), 10 µl GoTaq® Reaction buffer with 1.5 mM MgCl2 (1 x), 0.25 µl GoTaq® DNA polymerase (1.25 u) and DNase-, RNase-free filter-sterilized water (Sigma, Bornem, Belgium) to a final volume of 50 µl. Amplification conditions used were initial denaturation at 94 °C for 5 min; 35 cycles of denaturation at 94 °C for 1 min, annealing at 54 °C for 1 min, extension at 72 °C for 2 min; final extension at 72 °C for 12 min.

Denaturing gradient gel electrophoresis (DGGE) analysis

Ciliate DGGE analysis was performed using the Bio-Rad D gene system (Bio-Rad,hercules, CA). PCR fragments were loaded onto a 7% (w/v) polyacrylamide gel (77.8% acrylamide 40%, 22.2% bis-acrylamide 2%) in 1×TAE buffer (40 mM Tris, 20 mM acetate, 2 mM EDTA, pH 8.5) with denaturing gradient ranging from 40% to 60%. The electrophoresis was run for 16h at 60 °C and 45 V. DGGE patterns were visualized by staining with SYBR Green I nucleic acid gel stain (Molecular Probes, Eugene OR, USA). The obtained DGGE patterns were analysed with the BioNumerics software version 3.5 (Applied Maths, Kortrijk, Belgium). Similarities were calculated by the Pearson correlation, which takes into account band intensity and band position. The clustering algorithm of Ward was used to calculate dendrograms (Boeckaert et al., 2007).

Statistical analysis

Parameters were statistically analysed using a mixed model, with period and fat source (tallow, coconut, krabok oil) and cow as a fixed and random factor, respectively. Rumen fatty acid and qPCR data were analysed using the MIXED procedure using IBM SPSS Statistics 23 package. The model for the rumen fatty acid data included the fixed effect of day, time of sampling and their interaction and the random effect of cow assuming an autoregressive order one covariance structure fitted based on Akaike information and Schwarz Bayesian model fit criteria. The statistical model for qPCR data included the fixed effect of day and the random effect of cow assuming the covariance structure as described before. Least squares means are reported and significance was declared at $P<0.05$, and a trend at $0.05 \geq P<0.10$.

Results

Animals and feed intake

All the animals remained healthy throughout the experiment and consumed all their daily feed allocation (no feed refusals were collected). The average bodyweight of the animals for experimental period 1, 2 and 3 were 429, 415 and 422 kg, respectively.

Selected indices of rumen fermentation and protozoa counts

The concentration of total VFA (Table 3) was not affected ($P = 0.804$) by the diet. Except for propionic acid which showed a trend ($P = 0.056$), the proportions of the remaining VFA (Table 3) were not significantly ($P>0.05$) different between treatments. Also a trend ($P = 0.070$) was observed for the acetate to propionate ration to be lower after feeding of the TMR containing coconut oil compared to the other two diet. The KO diet had an acetate to propionate ration comparable to the T diet.

Total protozoa counts per unit rumen fluid were significantly ($P = 0.01$) affected by the dietary treatment. Compared to the T diet, the CO and KO diets had significantly reduced protozoa counts; 65% and 40%, respectively. Statistically significant differences, however, between the experimental rations could not be detected ($P = 0.448$) for the ciliates. There was however, a strong positive ($R^2 = 0.88$) linear ($y = 1.869x - 3.038$) association between the total protozoa counts (y) and ciliate numbers (x). There were no significant differences in the counts of amylolytic ($P = 0.472$), cellulolytic, ($P = 0.152$) and proteolytic ($P = 0.872$) bacteria (Table 3).

DGGE analysis

The DGGE profile of one sample of a cow fed the KO diet showed no ciliate communities to be present. The remaining eight DGGE profiles indicated two clusters of ciliate communities to be present (Figure 1). One cluster included all the T diet-fed animals while the other cluster contained all except one cow fed the KO diet.

https://doi.org/10.14456/jsat.2020.4

Table 3. Selected indices of rumen fermentation and protozoa counts after the feeding of the experimental rations.

Parameter	Experimental ration			SEM	P-value
	Tallow	Coconut oil	Krabok oil		
Total VFA (mmol/l)	70.4	71.9	73.3	3.1	0.804
Individual VFA (mol/100 mol)					
Acetic acid	66.7	62.8	64.9	1.2	0.131
Propionic acid	18.3$^{(b)}$	21.7$^{(a)}$	18.6$^{(b)}$	1.0	0.056
Butyric acid	11.9	12.6	13.8	0.9	0.343
Iso-valeric acid	0.20	0.17	0.15	0.30	0.563
Valeric acid	0.12	0.13	0.12	0.10	0.840
Acetate/propionate	3.70$^{(a)}$	3.00$^{(b)}$	3.54$^{(ab)}$	0.20	0.070
Microbiota					
Total protozoa (× 10^5 cell /ml)	5.09^{a}	1.80^{b}	3.04^{b}	0.38	0.010
Ciliates (log copy/g rumen fluid)	4.11	2.48	3.60	1.78	0.448
Amylolytic bacteria (× 10^7 cell/ml)	5.74	6.37	6.49	0.42	0.472
Cellulolytic bacteria (× 10^9 cell/ml)	6.73	7.28	7.69	0.27	0.152
Proteolytic bacteria (× 10^7 cell/ml)	4.87	5.54	5.74	0.36	0.872

^{a,b}Treatment means within the same row with different superscript are significantly different or show a trend (superscript between brackets) to differ (P<0.1).
VFA=volatile fatty acids.

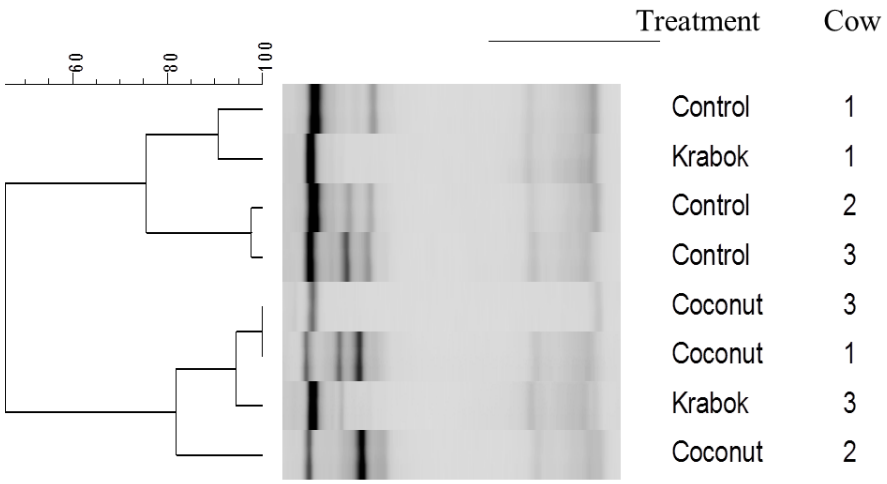

Figure 1. Cluster analysis of the of the denaturing gel electrophoresis profile of ciliate protozoa present in the rumen of beef cows fed a total mixed ration supplemented with either tallow (control), coconut oil or krabok oil+tallow.

Discussion

The present study indicates that coconut oil has a marked effect on numbers and the community of protozoa in the rumen. The number of protozoa decreased (P=0.010) by 65% and 40% in the CO and KO diet, respectively, when compared to the control. Similar effects of coconut oil and krabok oil have been reported by Panyakaew et al. (2013a), when higher amounts of C12:0+C14:0 (35 g/kg of supplemented fat) were fed to bulls. The latter authors found that the number of protozoa was decreased by 31 and 51%, respectively. Moreover, similar defaunating effects of coconut oil have been reported by Machmüller et al. (2003) and Machmüller (2006). A reduction in ciliate protozoa counts of 88 and 97% was reported by the latter author when 3.5 and 7.0% of coconut oil were added to a basal diet. An earlier study from the same group (Machmüller et al., 2003) reported a 65% decrease in ciliate protozoa numbers when sheep were fed with coconut oil instead of protected fat at 50 g/kg DM, double the amount used in the present study. Although protozoa numbers were decreased in the present study, ciliates were not affected (Table 3) due to high variability. However, there was a strong (R^2=0.88) positive linear association between total protozoa counts and the ciliate values.

The effect of coconut oil and krabok oil on the number of protozoa has been reported to be negatively correlated with propionate with krabok oil

https://doi.org/10.14456/jsat.2020.4

having more potential to reduce ruminal methanogenesis (Panyakaew et al., 2013b). In the present study, however, krabok versus coconut oil had a lesser potential to reduce the protozoa numbers, which agrees with the propionate levels being not affected by krabok oil. The difference in results between the two studies may be due to the difference in the dietary fat content which was ~ 30% lower the current study. The T diet in both studies yielded almost identical value for acetate and propionate concentration indicating that the differences were caused by coconut oil and krabok oil supplementation. The amounts of C12:0 and C14:0 supplemented in the present study were lower in both the C and KO diets indicating that reduction in the protozoa number is more sensitive in C12:0 than C14:0. This reasoning is in line with the *in vitro* results reported by Soliva et al. (1998). Moreover, the proportion of C12:0/C14:0 with twice of C (1:2.23) higher than KO (1:0.9) (calculated from table 2) diets in this studies, may cause of less effect of KO on the ciliate number and DGGE profile (Soliva et al., 2003; Dohme et al., 2001). From this result, it can be inferred that in practice a dose of, at least, 35 g of krabok oil per kg of diet should be used to reduced methane emission by beef cattle.

Unfortunately, one of the DGGE gels of a cow fed the KO diet did not yield valid results. The cluster analysis on the DGGE profiles of rumen ciliates showed two clusters of ciliate communities. One included all the T diet-fed animals and the other all the CO and KO diet-fed animals except one. The DGGE profiles indicate, therefore, that the supplementations of C12:0 + C14:0 affected ciliate communities. This is in line with the protozoa counts and the strong positive linear association between total protozoa counts and ciliate numbers. The DGGE profiles also corroborate the stronger effect of coconut oil compare to krabok oil on ciliate communities.

Conclusions

Krabok oil like coconut oil reduced the rumen protozoa population but both oils did not decrease ruminal ciliates numbers as measured by qPCR. The propionate proportion was only reduced by supplementation of coconut oil to the total mixed ration. Neither oils affected amylolytic, cellulolytic or proteolytic bacteria counts in the rumen fluid when supplementing the total mixed ration with 17 g/kg DM of total C10:0 + C12:0 + C14:0. Cluster analysis of the denaturing gel electrophoresis profile of ciliate communities showed a clustering of the coconut oil containing diet and the tallow containing diet. Coconut oil, and to a lesser extent krabok oil, affected the numbers of rumen protozoa.

Acknowledgements

This experiment was funded by the EU-community (project TH/Asia-Link/014-141-176) and the Laboratory of Microbial Ecology and Technology (LabMET), Faculty of Bioscience Engineering, Ghent University, Gent, Belgium.

Animal Welfare Statement

The authors confirm that the ethical policies of the journal, as noted on the journal's author guidelines page, have been adhered to and the appropriate ethical review committee approval has been received. The authors confirm that they have followed EU standards for the protection of animals used for scientific purposes.

References

Asanuma, N., Iwamoto, M., and Hino, T. 1999. Effect of the addition of fumarate on methane production by ruminal microorganisms *i n vitro*. J. Dairy Sci. 82, 780-787. DOI:10.3168/jds.S0022-0302(99)75296-3.

Boeckaert, C., Fievez, V., Vanhecke, D., Verstraete, W., and Boon, N. 2007. Changes in rumen biohydrogenation intermediates and ciliate protozoa diversity after algae supplementation to dairy cattle. Eur. J. Lipid Sci. Technol. 109, 767-777. DOI:10.1002/ejlt.200700052.

Boeckaert, C., Jouany, J.P., Lassalas, B., Morgavi, D.P., Vlaeminck, B., Boon, N., and Fievez, V. 2008. The rumen protozoon Isotricha prostoma and its associated bacteria play no major role in the biohydrogenation of linoleic acid. In *Gut microbiome: Functionality, Interaction with thehost and Impact on the Environment*. 6th INRA-RRI symposium, Clermont-Ferrand, France, p. 44. DOI:10.1017/S1751731109004285

Boon, N., Top, E.M., Verstraete, W., and Siciliano, S.D. 2003. Bioaugmentation as a tool to protect the structure and function of an activated-sludge microbial community against a 3-chloroaniline shock load. Appl. Environm. Microbiol. 69, 1511-1520. DOI: 10.1128/AEM.69.3.1511-1520.2003

Dohme, F., Machmüller, A., Estermann, B.L., Pfister, P., Wasserfallen, A., and Kreuzer, M., 1999. The role of the rumen ciliate protozoa for methane suppression caused by coconut oil. Lett. Appl. Microbiol. 29, 187-192. DOI:10.1046/j.1365-2672.1999.00614.x

Dohme, F., Machmüller, A., Wasserfallen, A., and Kreuzer, M. 2001. Ruminal methanogenesis as influenced by individual fatty acids supplemented to complete ruminant diets. Lett. Appl. Microbiol. 32, 47-51. DOI: 10.1046/j.1472-765x.2001.00863.x

Finlay, B.J., Esteban, G., Clarke, K.J., Williams, A.G., Embley, T.M., and hirt, R.P. 1994. Some rumen ciliateshave endosymbiotic methanogens. FEMS Microbiol. Lett. 117, 157-162. DOI: 10.1111/j.1574-6968.1994.tb06758.x

Galyean, M., 1989. Laboratory Procedure in Animal Nutrition Research. 1st edn., Department of Animal and Life Science, New Mexico States University, USA., pp. 162-167.

https://doi.org/10.14456/jsat.2020.4

Goel, G., Arvidsson, K., Vlaeminck, B., Bruggeman, G., Deschepper, K., and Fievez, V. 2009. Effects of capric acid on rumen methanogenesis and biohydrogenation of linoleic and alpha-linolenic acid. Animal 3, 810-816. DOI: 10.1017/S1751731109004352.

Guyader, J., Eugene, M., Noziere, P., Morgavi, D.P., Doreau, M., and Martin, C. 2014. Influence of rumen protozoa on methane emission in ruminants: a meta-analysis approach. Animal 8, 1816-1825. DOI: 10.1017/S1751731114001852

Hobson, P.N. 1969. Rumen bacteria. In Methods in Microbiology, Vol. 3B, eds. J.R. Norris and D.W. Ribbons. Academic Press, London, pp.133-149.DOI :10.1007/BF01576265.

Hook, S.E., Wright, A.D.G., and Mcbride, B.W. 2010. Methanogens: methane producers of the rumen and mitigation strategies. Archaea, 11p. DOI: 10.1155/2010/945785.

Hungate, R.E., 1969. A roll tube method for cultivation of strict anaerobes. Meth. Microbiol. 3, 117-132. DOI: 10.1038/d42859-019-00007-1.

Jordan, E., Lovett, D.K., Monahan, F.J., Callan, J., Flynn, B., and O'Mara, F.P. 2006. Effect of refined coconut oil or copra meal on methane output and on intake and performance of beef heifers. J. Anim. Sci. 84, 162-170. DOI: 10.2527/2006.841162x

Kreuzer, M. 1986. Methodik und anwendung der defaunierung beim wachsenden wiederkäuer. J. Vet. Med. 33A, 721-745. DOI: 10.1111/j.1439-0442.1986.tb00586.x

Lila, Z.A., Mohammed, N., Ksanda, S., Kamada, T., and Itabashi, H. 2003. Effect of sarsaponin on ruminal fermentation with particular reference to methane production *in vitro*. J. Dairy Sci. 86, 3330-3336. DOI: https://doi.org/10.3168/jds.S0022-0302(03)73935-6

Machmüller, A., and Kreuzer, M. 1999. Methane suppression by coconut oil and associated effects on nutrient and energy balance in sheep. Can. J. Anim. Sci. 79, 65-72.https://doi.org/10.4141/A98-079

Machmüller, A., Soliva, C.R., and Kreuzer, M. 2003. Effect of coconut oil and defaunation treatment on methanogenesis in sheep. Reprod. Nutr. Develop. 43(1), 41-55. Machmüller, A. 2006. Medium-chain fatty acids and their potential to reduce methanogenesis in domestic ruminants. Agricul. Ecosys. Environm. 112, 107-114.

Panyakaew, P., Goel, G., Lourengo, M., Yuangklang, C., and Fievez, V. 2013a. Medium-chain fatty acids from coconut or krabok oil inhibit *in vitro* rumen methanogenesis and conversion of non-conjugated dienoic biohydrogenation intermediates. Anim. Feed Sci. Technol. 180, 18-25. https://doi.org/10.1016/j.anifeedsci.2012.12.005.

Panyakaew, P., Goel, G., Yuangklang, C., Boon, N., Schonewille, J. Th.,hendriks, W.H., and Fievez, V. 2013b. Effect of supplementing coconut or krabok oil, rich in medium chain fatty acids on ruminal fermentation, protozoa and archaeal population of bulls. Animal, 1950-1958. https://doi.org/10.1017/S1751731113001766.

Van Ranst, G., Fievez, V., Vandewalle, M., Van Waes, C., De Riek, J., and Van Bockstaele, E. 2010. Influence of damaging and wilting red clover on lipid metabolism during ensiling and *in vitro* rumen incubation. Anim. Sci. 4, 1528-1540. DOI: 10.1017/S1751731110000625.

Soliva, C.R., Hindrichsen, I.K., Meile, L., Kreuzer, M., and Machmüller, A. 2003. Effects of mixtures of lauric and myristic acid on rumen methanogens and methanogenesis in vitro. Lett. Appl. Microbiol. 37, 35-39. DOI: 10.1046/j.1472-765x.2003.01343.x

Wongsuthavas, S., Yuangklang, C., Wittayakun, S., Vasupen, K., Mitchaothai, J., Srenanul, P., and Beynen, A.C. 2007. Dietary soybean oil, but not krabok oil, diminishes abdominal fat deposition in broiler chickens. Poultry Sci. 6, 792-795. DOI: 10.3923/ijps.2007.792.795.

Yu, Z., and Morrison, M. 2004. Comparisons of Different Hypervariable Regions of rrs Genes for Use in Fingerprinting of Microbial Communities by PCR-Denaturing Gradient Gel Electrophoresis. Appl. Environ. Microbiol. 7, 4800-4806. DOI: 10.1128/AEM.70.8.4800–4806.2004

JSAT
Journal of Science and Agricultural Technology
Research Article
https://doi.org/10.14456/jsat.2020.5
e-ISSN 2730-1532, ISSN 2730-1524

Preparation of activated carbon as support of nickel catalyst for Guerbet reaction

Krittanun Deekamwong[1], Supunnee Junpirom[2] and Jatuporn Wittayakun[1]*

[1] School of Chemistry, Institute of Science, Suranaree University of Technology, Nakhon Ratchasima, 30000 Thailand
[2] School of Chemical Engineering, Institute of Engineering, Suranaree University of Technology, Nakhon Ratchasima, 30000 Thailand

***Corresponding author**: *jatuporn@sut.ac.th*
Received January 22, 2020. Revised March 27, 2020. Accepted March 29, 2020.

Abstract

This work aims to prepare activated carbon from charcoal from the wood of *Muntingia calabura Linn*. and employ as support for nickel catalyst. The charcoal was obtained from an Iwasaki kiln and activated by CO_2. Then, the surface of activated carbon was modified by air zero to create acid functional groups. The polyaromatic-like structure and functional groups of the activated carbon were characterized by Fourier transform infrared spectroscopy (FTIR) and elemental analysis. The thermal stability was carried out by thermogravimetric analysis (TGA). The surface areas of the samples were determined by Brunauer–Emmett–Teller (BET) from N_2 adsorption-desorption analysis. The activated carbon after modification had higher acid functional groups than the parent charcoal. The BET surface area decreased after modification, but the thermal stability did not change after CO_2 treatment. After impregnated with nickel precursor, the phases of the catalyst were analyzed by X-ray diffraction (XRD). Nickel nanoparticles were produced on activated carbon. The catalytic screening of Guerbet reaction to produce *n*-butanol from ethanol conversion was performed under autogeneous pressure at 240 °C for 6 h. The nickel supported on activated carbon showed higher ethanol conversion than the unsupported nickel nanoparticles.

Keywords: *Muntingia calabura Linn*.; activated carbon; nickel nanoparticles, catalyst, guerbet reaction

Introduction

It is possible that *n*-butanol could become a part of biofuels, especially for transportation according to its high heating value, high flash point, low oxygen content and miscibility with diesel and gasoline. Currently, a commercial method to produce *n*-butanol is fermentation from food. However, the production capacity, competition with food and toxicity from bacteria are concerned (Kaminski et al., 2011). The research process is shifted to a chemical reaction of ethanol from biomass in the presence of a heterogeneous catalyst. Riittonen et al. (2012) have studied a one-pot liquid-phase reaction. They have concluded that Ni metallic form supported on Al_2O_3 (Ni/Al_2O_3) shows a better catalytic activity than the supported Pt, Pd, Ag and Co. Then, Zhang et al. (2013) have revealed a simple and environmentally friendly method to produce *n*-butanol by Guerbet process (see equation below) with Co metal powder in a hydrothermal batch reactor at 240 °C and autogenous pressure; a good yield and high selectivity are obtained. Although a good reaction pathway of *n*-butanol is developed (Zhang et al., 2013), the catalyst is still expensive. This problem could be solved by dispersing the metal active phase on porous materials.

Guerbet process:

$$2CH_3CH_2OH \rightarrow CH_3CH_2CH_2CH_2OH + H_2O$$

Activated carbon is a porous material which is widely used as a support for nickel catalyst (Fidalgo et al., 2010; Rios et al., 2003; Vasu et al., 2008; Wojcieszak et al., 2006; Yao et al., 2008). Thus, nickel on activated carbon could give high nickel active sites. This property could help to upgrade the catalytic activity on the Guerbet process.

Activated carbon is widely used as catalyst support because it has a high surface area, acid/base resistivity and low cost of production. Typically, the activated carbon is prepared from a lignocellulosic material by pyrolysis and physical/chemical treatment. The layers of the polyaromatic-like molecules contain acid/base functional groups. Junpirom et al. (2007) have investigated the surface modification by chemical and physical treatment. The physical treatment by air zero is a suitable and environmentally friendly method to increase the acid sites on the activated carbon surface. Those acid functional groups are adsorption sites for cation (Azzi Rios et al., 2003; Vasu et al., 2008). Then, the cations could be reduced to form nanoparticles on activated carbon.

https://doi.org/10.14456/jsat.2020.5

The goal in this work is to prepare activated carbon for the application as catalyst support. First, the wood of *Muntingia calabura Linn*., a local plant from Nakhon Ratchasima province, Thailand, was pyrolyzed in an Iwasaki kiln to produce charcoal. Then, the charcoal was activated by carbon dioxide (CO_2) in a horizontal tube furnace. Finally, the activated carbon is used as a support for nickel catalyst for the synthesis of *n*-butanol from ethanol via the Guerbet process in a batch reactor under autogenous pressure at 240 °C.

Experimental

Preparation of charcoal in an Iwazaki kiln

The wood of *Muntingia calabura Linn*. with diameter of about 5-10 cm was collected from a local field near the university. It was cut to the length of about 80 cm and dried in air under sunlight for 30 days. The pyrolysis of *Muntingia calabura Linn.* wood was carried out in an Iwazaki kiln (Figure 1) at Energy Ashram, Appropriate Technology Association in Pakchong District, Nakhon Ratchasima. The furnace was built with a 200-litre oil tank connected with an asbestos tube and steel condenser. The optimum temperature and airflow were controlled by adjusting a gap in the front of the furnace. After about 10 h, the gap was closed and the furnace was cooled down to ambient temperature. The obtained charcoal was collected.

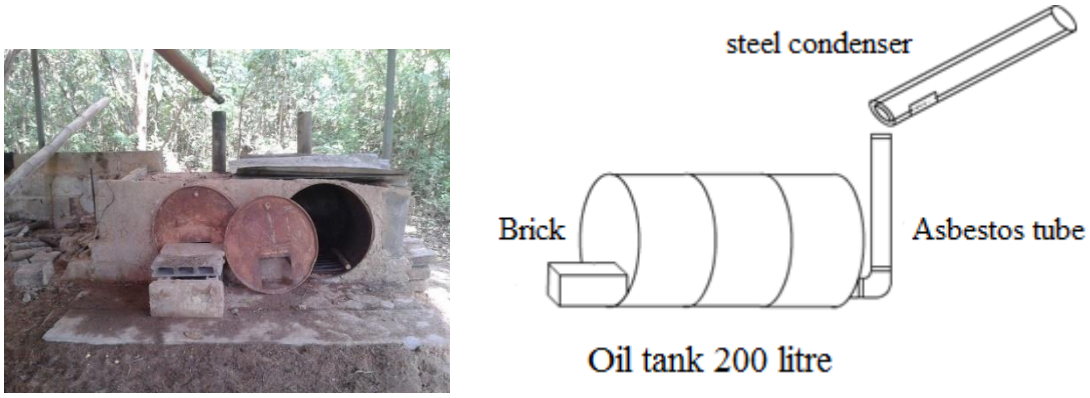

Figure 1. (Left) The actual Iwazaki kiln (Right) drawing to represent the parts.

Preparation of activated carbon by CO_2 physical treatment

The charcoal of *Muntingia calabura Linn*. was activated by CO*2* physical treatment in the horizontal tube furnace (Carbolite, UK) with a length of 122.2 cm and internal diameter of 3.8 cm (Junpirom et al., 2007). In each preparation, about 2 g of charcoal was crushed and sieved to average particle sizes between 2.1 mm – 0.714 µm, loaded in two ceramic boats and placed at the center of the furnace. It was heated from room temperature to 800 °C with a heating rate of 20 °C/min under N_2 flow (100 mL/min) followed by CO_2 flow (100 mL/min, Linde Gas, 99.95%) for 1 h. Finally, the furnace was turned off and cooled to the ambient temperature under N_2 flow. The obtained sample was named "AC".

Modification of activated carbon surface by air zero physical treatment

The surface of activated carbon was modified by physical treatment in the horizontal tube furnace (Junpirom et al., 2007). In each preparation, about 2 g of activated carbon was crushed and sieved to average particle sizes between 2.1 mm – 0.714 µm, loaded in two ceramic boats and placed at the center of the furnace. It was heated from room temperature to 250 °C with a heating rate of 20 °C/min under N2 flow (100 mL/min) followed by air zero (100 mL/min, 21% O_2 in N2 balance) flow for 24 h. Finally, the furnace was turned off and cooled to the ambient temperature under N_2 flow. The obtained sample was named "Mod AC".

Characterization of activated carbon and modified activated carbon

Functional groups of samples were determined by Fourier transform infrared spectroscopy (FTIR, Perkin Elmer, Spectrum GX). N_2 adsorption-desorption isotherm was obtained from a Micromeritics ASAP 2010. The surface area was calculated by the Brunauer–Emmett–Teller (BET) method. Thermal stability of the material was investigated by thermogravimetric and differential

https://doi.org/10.14456/jsat.2020.5

thermogravimetric analysis (TGA-DTA, TA Instrument/ SDT2960) under N_2 at the flow rate of 100 mL/min. The sample was heated from 40 to 900 °C at a heating rate 20 °C /min". The chemical composition was determined by CHNO elemental analysis (Leco, TruSpec Micro CHNO).

Synthesis of nickel nanoparticle

Nickel nanoparticles were synthesized by a method modified from Zhang et al. (2004) and Motuzas et al. (2014). A mixture with OH^-:Ni^{2+} at the molar ratio of 4:1 was prepared by dissolving from 0.3553 g of nickel acetate tetrahydrate (98+%, Strem chemicals) and 2.2373 g of sodium hydroxide (technical grade, Carlo Erba) in 60 mL of ethylene glycol (technical grade, Carlo Erba). The resulting solution was transferred into a 100 mL microwave vessel, closed and heated via microwave irradiation in a Microwave MARs 6-One Touch in which the temperature is monitored by IR sensor with adjustable power output (300 W). The solution was heated with the rate of 5 °C/min to 180 °C and held at the final temperature for 15 min. After cooling to room temperature, the precipitate was filtered, washed with ethanol and dried at 160 °C overnight. The obtained sample was named "Nickel nanoparticle."

Preparation of nickel supported on modified activated carbon by precipitation (Ni/Mod AC)

One gram of modified activated carbon was dispersed in a 0.3553 g of nickel acetate tetrahydrate in 30 mL of ethylene glycol to allow nickel to adsorb on the surface for 12 h. Then, 2.2373 g of sodium hydroxide in 30 mL of ethylene glycol producing the OH^-:Ni^{2+} at the molar ratio of 4:1 was added. The 10% w/w of Ni^{2+} was expected. The resulting solution with the total volume of 60 mL was transferred into a 100 mL microwave vessel, closed and heated via a Microwave MARs 6-One Touch. The solution was heated with the rate of 5 °C/min to 180 °C and held at the final temperature for 15 min. After cooling to room temperature, the precipitate was filtered, washed with ethanol and dried at 160 °C. The obtained sample was named "Ni/Mod AC."

Characterization of nickel nanoparticle and Ni/Mod AC

Nickel nanoparticle and Ni/Mod AC was characterized by X-ray diffraction (XRD, Bruker D8 Advance), generating Cu-K_α radiation operating at a voltage of 40 kV and current of 40 mA. The crystalline size (D) was calculated by using the Scherrer's equation (Equation 1)

$$D = \frac{0.89\lambda}{\beta\cos\theta} \quad (1)$$

where λ is wavelength (1.5418 Å), β is full width at half maximum (FWHM) of the peak and θ is the Bragg's angle of the XRD peak from the main diffraction peak. Functional group was analyzed by FTIR.

Catalytic performance on hydrothermal synthesis of *n*-butanol from ethanol

Catalytic reaction was done in a 450 mL of Parr 5500 compact reactor with the following procedure. The starting reagent solution containing 150 mL of ethanol (absolute, Carlo Erba), 4.2 g of $NaHCO_3$, 70 mL of water and 0.4 g of catalyst was added into the autoclave, sealed, placed in a furnace and heated to 240 °C for 6 h. The final autogenous pressure in the autoclave was around 55 bars as measured by a digital pressure gauge. After each test, the autoclave was quenched to room temperature by water-cooling.

Products were analyzed by a gas chromatograph equipped with flame ionization detector (GC-FID, Agilent G1530A) equipped DB-wax (polyethylene glycol) column. The 0.5 mL of sample and 0.1 mL of *n*-heptanol as an internal standard were diluted in 25 mL of water. The sample (0.1 µL) was injected with a 50:1 split mode. The injection and FID detector temperature were 180 °C and 100 °C, respectively. The temperature was programmed from 100 °C, ramp to 120 °C at 4 °C/min and then to 180 °C at 30 °C/min for 1 min.

The concentration of ethanol was determined from a standard curve produced by the ratio of peak height of ethanol and *n*-heptanol with various %v/v of ethanol. Then the conversion of ethanol was calculated by Equation 2 (Riittonen et al., 2015):

$$\text{Conversion of ethanol } (\%) = \left(\frac{C_0 - C_i}{C_0}\right) \times 100 \quad (2)$$

where C_0 is the initial concentration of ethanol and C_i is measured concentration of ethanol after catalytic reaction. The *n*-butanol selectivity was estimated from the ratio of the peak height of *n*-butanol and *n*-heptanol.

Results and discussion

Characterization of charcoal, activated carbon and modified activated carbon

The FTIR spectra of the charcoal, AC and Mod AC and peaks assignment are shown in Figure2. From the charcoal sample, the bands corresponding to C–C aromatic carbon of polyaromatic-like structure and O–H bond were observed. After activation, the band corresponding to carbonyl

https://doi.org/10.14456/jsat.2020.5

groups was observed and the C–C bond was retained (Hesas et al., 2013). Then, the O-H groups were displayed together with carbonyl groups in Mod AC (Hesas et al., 2013). Moreover, all samples showed C=N bond (Aboud et al., 2015). Therefore, the C–OH was transformed to C=O after activation and then converted to COOH after surface modification regarding to the presence of both C=O and C–OH functional groups.

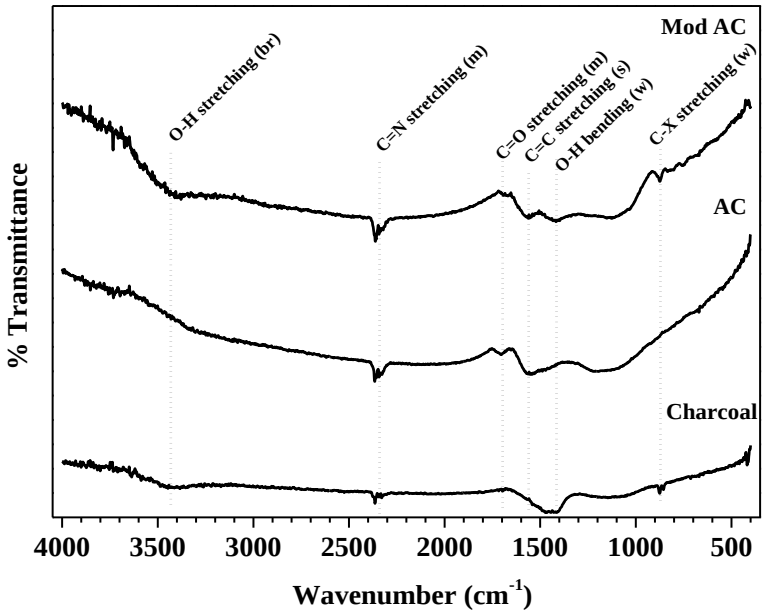

Figure 2. FTIR spectra of charcoal, AC and Mod AC; Intensity: br=broad, w=weak, m=medium and s=strong.

The elemental compositions of the charcoal, AC and Mod AC are shown in Table 1. The major component is carbon, followed by oxygen and trace of hydrogen and nitrogen. The carbon to oxygen (C/O) ratio implies the high amount of acid site. After activation and modification, the oxygen content increased indicating that the approximated acid sites were increased (Ngernyen et al., 2005).

Table 1. Elemental composition of charcoal, AC and Mod AC.

	C (%)	H (%)	N (%)	O (%)	C/O
Charcoal	83.185	2.929	0.792	6.294	13.22
AC	82.284	1.531	1.180	10.680	7.705
Mod AC	74.790	2.492	0.737	10.090	7.412

The TGA thermogrgams and % weight derivatives of AC and Mod AC are shown in Figure 3. The first weight loss at below 100 °C corresponded to removal of physisorbed water. The second weight loss between 100 – 700 °C referred to the decomposition of the surface functional group. The last weight loss at the temperature about 700 °C corresponded to the decomposition of activated carbon (Peng et al., 2014). The gradual weight loss probably attributed to the decomposition of surface functional groups. According to the weight change, the AC and Mod AC were thermally stable up to 400 °C and 550 °C, respectively. Thus, both samples were suitable as catalyst supports for a reaction condition below those temperatures.

N_2 adsorption-desorption isotherms of AC and Mod AC are shown in Figure 4 The adsorption at $P/P_0 < 0.1$ corresponded to monolayer adsorption (Hesas et al., 2013). The BET surface area of the AC was 412 $m^2.g^{-1}$. After modification, Mod AC had a lower volume adsorbed (V_a) and the BET surface area was 170 $m^2.g^{-1}$. The modification could cause the collapse of pores. It was also possible that the presence of functional groups, such as hydroxyl and carboxyl blocked N_2 to enter the pore (Ngernyen et al., 2005).

https://doi.org/10.14456/jsat.2020.5

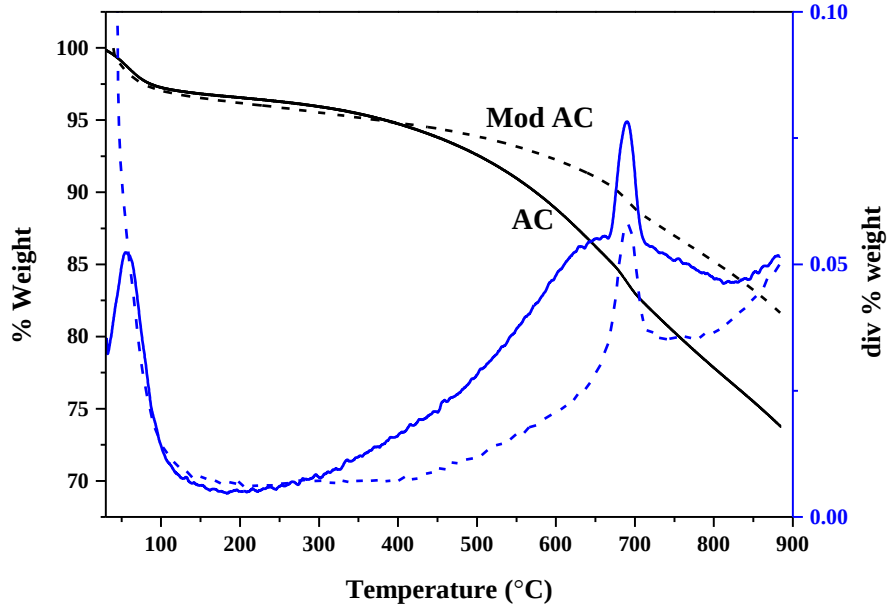

Figure 3. TGA Thermograms and % weight derivatives of AC (solid line) and Mod AC (dashed line).

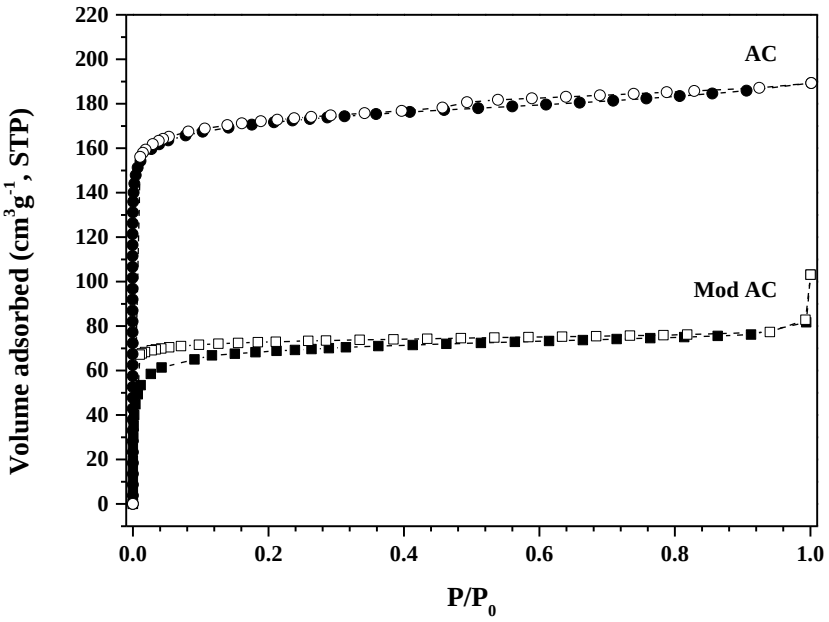

Figure 4. N2 adsorption-desorption isotherms of AC and Mod AC; adsorption (filled) and desorption (empty).

The XRD pattern of nickel nanoparticles is shown in Figure 5. The main diffraction peaks at 44.4, 51.8 and 76.2 degree were assigned to (100), (200) and (220) planes of metallic nickel form, respectively (Zhang et al., 2004). The sample did not show the peaks at 32.9, 38.5 and 51.7 degree corresponding to $Ni(OH)_2$ as intermediate phase and the peaks at 37.2, 43.3 and 62.9 degree corresponding to NiO (Motuzas et al., 2014; Dharmaraj et al., 2006). Nickel nanoparticles were synthesized successfully at 180 °C in 15 min. Thus, the crystalline size calculated by Scherrer's equation was about 32 nm with 0.46 degree of FWHM. The method to synthesize nickel nanoparticle was improved by using a shorter time and lower temperature than that of the original method (Motuzas et al., 2014; Zhang et al., 2004).

The XRD pattern of nickel phase on modified activated carbon is shown in Figure 5. Nickel XRD pattern was similar to nickel nanoparticle. The crystalline size was about 50 nm by Scherrer's equation with 0.30 degree of FWHM.

https://doi.org/10.14456/jsat.2020.5

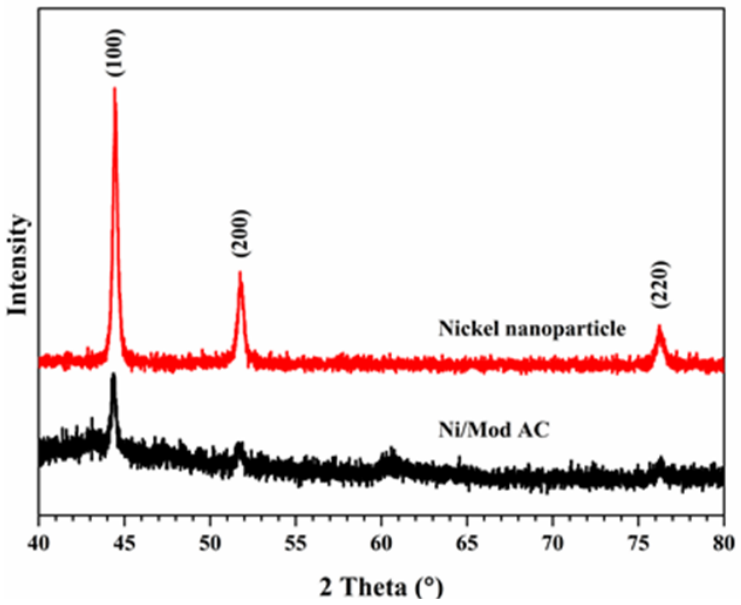

Figure 5. XRD patterns of nickel nanoparticles and Ni/Mod AC.

Catalyst screening on Guerbet reaction

Before catalytic testing, a blank test was carried out with the absence of a catalyst. The ethanol conversion was obtained (see Table 2). The $NaHCO_3$ in the solution could serve as a base catalyst to convert ethanol to acetaldehyde, butyraldehyde, crotonaldehyde, crotylalcohol, 2-butanol and *n*-butanol (Ndou et al., 2003).

By using 1 g of nickel nanoparticle catalyst, the ethanol conversion was more than two-fold higher than the blank test. Therefore, the nickel catalyst could be a hydrogen borrowing for dehydrogenation and hydrogenation. Both reactions produced two molecules of aldehyde (intermediate), butanal (intermediate) and butanol (Riittonen et al., 2012; Zhang et al., 2013). The ethanol conversion of Mod AC slightly increased compared to the blank test. However, there was no evidence to confirm the connection of these phenomena to the role of the bare supports.

The catalytic testing of nickel impregnated on Mod AC was carried out to see effect of metal dispersion. The supported catalyst showed a higher ethanol conversion than the nanoparticles. The role of support material on nickel catalyst resulted to improve catalytic conversion. The approximated *n*-butanol selectivity was the highest from nickel nanoparticle. However, the selectivity from Ni-Mod AC was higher than that from the parent support because of the presence of nickel nanoparticles. The lower selectivity might imply that the side reactions happened by the imbalance of acidic and basic catalysts of support and $NaHCO_3$ (Jordison et al., 2015).

Table 2. Ethanol conversion (%) and peak area of *n*-butanol fom the catalyst screening determined from GC-FID technique.

Catalyst	Ethanol conversion (%)		Peak area of *n*-butanol
		Per mmole of Ni	
None	6.1	-	0.071
Nickel nanoparticle	15.9	2.3	0.50
Mod AC	8.7	-	0.098
Ni/Mod AC	19.2	28.2	0.103

https://doi.org/10.14456/jsat.2020.5

Conclusions

Activated carbon was prepared from charcoal of *Muntingia calabura Linn.* wood by CO_2 physical treatment. Regarding FTIR and CHNO analysis, oxygen-containing functional groups referred to acid sites increased after activation and modification. Both AC and Mod AC showed high thermal stability. However, the surface area of modified activated carbon decreased because of pore-blocking by the presence of the functional group. Then, nickel catalyst (Ni/Mod AC) was prepared by dispersion of nickel nanoparticles on the Mod AC. The activity of *n*-butanol synthesis from ethanol conversion via Guerbet process was lower than that from other works. However, the multifunctional active site containing metal and acid/base is promising to improve the catalytic reaction.

Acknowledgement

This work is supported by Suranaree University of Technology. A scholarship for K. Deekamwong is from the Thai government under the Development and Promotion of Science and Technology Talents (DPST) Project.

References

Aboud, M.F.A., ALOthman, Z.A., Habila, M.A., Zlotea, C., Latroche, M. and Cuevas, F. 2015. Hydrogen storage in pristine and d10-block metal-anchored activated carbon made from local wastes. Energies. 8: 3578 – 3590.

Azzi Rios, R.R.V., Alves, D.E., Dalmázio, I., Bento, S.F.V., Donnici, C.L. and Lago, R.M. 2003. Tailoring Activated Carbon by Surface Chemical Modification with O, S, and N Containing Molecules. Materials Research. 6(2): 129 – 135.

Dharmaraj, N., Prabu, P., Nagarajan, S., Kim, C.H., Park, J.H. and Kim, H.Y. 2006. Synthesis of nickel oxide nanoparticles using nickel acetate and poly(vinyl acetate) precursor. Materials Science and Engineering: B. 128(1-3): 111 – 114.

Fidalgo, B., Zubizarreta, L., Bermúdez, J.M., Arenillas, A. and Menéndez, J.A. 2010. Synthesis of carbon-supported nickel catalysts for the dry reforming of CH4. Fuel Processing Technology. 91: 765 – 769.

Hesas, R.H., Arami-Niya, A., Daud, W.M.A.W. and Sahu, J.N. 2013. Preparation and characterization of activated carbon from apple waste by microwave-assisted phosphoric acid activation: application in methylene blue adsorption. BioResources. 8(2): 2950 – 2966.

Jordison, T.L., Lira, C.T. and Miller D.J. 2015. Condensed-phase ethanol conversion to higher alcohols. Industrial & Engineering Chemistry Research. 45: 10991 – 11000.

Junpirom, S., Tangsathitkulchai, C. and Tangsathitkulchai, M. 2007. Preparation of activated carbons from longan seed by physical and chemical methods (in Thai). Suranaree Journal of Science and Technology. 14(1): 63 – 76.

Kamiński, W., Tomczak, E. and Górak, A. 2011. Biobutanol - production and purification methods. Ecological Chemistry and Engineering S. 18: 31 – 37.

Motuzas, J., Drobek, M., Diniz da Costa, J.C. and Julbe, A. 2014. Novel microwave assisted approach to large scale nickel nanoparticle fabrication. Chemical Engineering Journal. 240: 155 – 160.

Ndou, A.S., Plint, N. and Coville, N.J. 2003. Dimerisation of ethanol to butanol over solid-base catalysts. Applied Catalysis A: General. 251: 337 – 345.

Ngernyen, Y., Tangsathitkulchai, C. and Tangsathitkulchai, M. 2005. The modification of acidic surface functionality of wood-based activated carbon. Suranaree Journal of Science and Technology.

Peng, G., Steib, M., Gramm, F., Ludwig, C. and Vogel, F. 2014. Synthesis factors affecting the catalytic performance and stability of Ru/C catalysts for supercritical water gasification. Catalysis Science & Technology. 4(9): 3329 – 3339.

Riittonen, T., Eränen, K., Mäki-Arvela, P., Shchukarev, A., Rautio, A.-R., Kordas, K., Kumar, N., Salmi, T. and Mikkola, J. 2015. Continuous liquid-phase valorization of bio-ethanol towards bio-butanol over metal modified alumina. Renewable Energy. 74: 369 – 378.

Riittonen, T., Toukoniitty, E., Madnani, D.K., Leino, A.-R., Kordas, K., Szabo, M., Sapi, A., Arve, K., Wärnå, J. and Mikkola, J.-P. 2012. One-pot liquid-phase catalytic conversion of ethanol to 1-butanol over aluminium oxide - the effect of the active metal on the selectivity. Catalysts. 2: 68 – 84.

Rios, R.R.A., Alves, D.E., Fernando, D.S., Bento, V., Donnici, L. and Lago, R.M. 2003. Tailoring Activated Carbon by Surface Chemical Modification with O, S, and N Containing Molecules. Material research. 6: 129 – 135.

Vasu, A.E. 2008. Surface Modification of Activated Carbon for Enhancement of Nickel(II) Adsorption. E-Journal of Chemistry. 5(4): 814 – 819.

Wojcieszak, R., Zieliński, M. and Bettahar, M.M. 2006. Study of nickel nanoparticles supported on activated carbon prepared by aqueous hydrazine reduction. Journal of Colloid Interface Science. 299(1): 238 – 248.

Yao, S., Yang, C., Tan, Y. and Han, Y. 2008. Deactivation and regeneration of an activated carbon-supported nickel catalyst for methanol carbonylation in the vapor phase. Catalysis Communications. 9(11–12): 2107 – 2111.

Zhang, F., Chen, Y., Zhao, J. and Li, H. 2004. Preparation of Nanosized Nickel Particles by Hydrothermal Method. Chemistry Letters. 33(2): 146 – 147.

Zhang, X., Liu, Z., Xu, X., Yue, H., Tian, G. and Feng, S. 2013. Hydrothermal synthesis of 1-butanol from ethanol catalyzed with commercial cobalt powder. ACS Sustainable Chemistry & Engineering. 1: 1493 – 1497.

INSTRUCTION FOR AUTHORS

1. Types of articles and formats

Manuscripts may be submitted to JSAT in the form of Review Articles or Research Articles and must be clearly and concisely written in English with appropriate pages.

2. Preparation of manuscripts

All manuscripts must be prepared and submitted as single Word file (.docx) (Word 2007 or higher). For English font, please use "Time New Roman" with text size of 12 point. Please prepare your manuscript in double-space on A4-sized page. Line number must be used continuous numbering in manuscript. The submitted manuscript should be organized as follow:

2.1) Title

The title of manuscript should be supplied with enough information to catch the attention of readers.

2.2) Author names and affiliations

Please clearly indicate the given name(s) and family name(s) of each author and check that all names are accurately spelled. Indicate the corresponding author by "*". If authors have different addresses, numbered superscripts are required to refer to each address provided. The format of authors' affiliations should be: 1. Department, University, City name, State name, Postal code and Country. Corresponding author must inform email.

2.3) Abstract and keywords

Abstract - A concise abstract with maximum of 200-250 words identifying the new and significant results of the study must be provided for all manuscripts. Keywords: – At least 3 to 5 keywords must be given below abstract and use "comma (,)" to separate each.

2.4) Introduction

Author should prepare the introduction with suitable length and keep it as short as possible.

2.5) Materials and methods

This section contains details about materials, techniques, apparatuses, experimental design, and environment. Sufficient detail should be provided to permit the reader to repeat the experiments. For the manuscript reports the utilization of chemical, please provide the purity of all chemicals used in this part.

2.6) Results and discussion

In this part, the results and discussion can be combined or separated depends on author design. Please use tables, graphs, diagrams, and photographs to provide a clear understanding of the results. Quantitative measures of significance (P-values) should be presented. Authors may use either absolute P-values or a defined significance level as long as usage is consistent. Discussion contains the interpretation of the results into existing literature. It should be clear and concise, address the related mechanisms and their significance.

2.7) Conclusions

Clear and significant conclusions should be provided and related to the results and objectives of your work.

2.8) Acknowledgement

In this section, financial and material support should also be mentioned. Authors should list all funding sources in this acknowledgments section. The names of funding organizations should be written in full. List those individuals who provided support during the research

2.9) References

2.9.1) In text citations, please use name-year system such as:

a. Before texts: Smith (2018)…., Tsuji and Hayate (2012)…., Smith et al.(2019)…., Smith (2018); Tsuji (2012)…., Smith et al.(2018a); Smith et al.(2018b)…..

b. After texts: …. (Smith, 2018), …. (Tsuji and Hayate, 2012), …. (Smith et al., 2019), …. (Smith, 2018; Tsuji, 2012), …. (Smith et al., 2018a; Smith et al., 2018b)

2.9.2) References list

Published literatures or unpublished works must be listed alphabetically by surname of author at the end of the manuscript. Each reference to a periodical publication must include, in order, the name(s) of the author(s), the year of publication, the full title of the article, the publication in which

it appears, the volume and inclusive page numbers, and the digital object identifier (DOI), if available. Examples of references are listed as follow:

• Journal article

Halmilton, M.B., Pincus, E.L., Fion, A.D., and Fleischer, R. C. 1999. Universal linker and ligation procedures for construction of genomic DNA libraries enriched for microsatellites. Biotechniques. 27: 500-507. https://doi.org/xx.xxxxxxxxxx Gupta, A.P., and Kumar, V. 2007. New emerging trends in synthetic biodegradable polymers-polylactide: A critique. European Polymer Journal. 43: 4053-4074.

• Book

Carr, R.L. 1976. Powder and granule properties and mechanics. Marcel Dekker Publisher, New York.

• Chapter in book

Jackson, M.B. 1982. Ethylene as a growth promoting hormone under flooded conditions. In: Wareing, P.F. (ed) Plant growth substance. Academic Press, London. p.291-301.

• Proceeding, symposia etc.

Pratt, A., Gilkes, R.J., Ward, S.C., and Jasper, D.A. 2000. Variations in the properties of regolith materials affect the performance of tree growth in rehabilitated bauxite mine-pits in the Darling Range, SW-Australia. In: Brion, A., and Bell, R.W. (eds) Proceeding of Remade Land 2000, the International Conference on Remediation and Management of Degraded Lands. Fremantle, 30 Nov-2 Dec 2000. Promaco Conventions, Canning Bridge. p.87-88.

• Dissertation

Senthong, C. 1979. Growth analysis in several peanut cultivars and the effect of peanut root-knot nematode (Meloidogyne arenaria) on peanut yields. Ph.D. Dissertation. University of Florida, Gainesville, Florida, USA.

3. Equation, figure, table and unit of measurement

Equation

All equations presented in the text can be prepared by Equation editor from Microsoft word or Math Type.

Figure

Data presented in figure must be written in English. Color or gray scale figure should be prepared as TIFF format (.tif) with at least 600 dpi. Photograph should be prepared as TIFF (.tif) or JPEG (.jpg) format with at least 600 dpi. Figure with caption should be placed next to the relevant text, rather than at the bottom of the file.

Table

Data presented in table must be written in English. Table with caption and footnote should be placed next to the relevant text, rather than at the bottom of the file.

Unit

Author should use the International System of Units (S.I.)

4. Structure of manuscript

- Title
- Author names and affiliations
- Abstract
- Keywords
- Introduction
- Materials and methods
- Results and discussion

- Conclusion
- Acknowledgement (if any)
- References

5. After acceptance

Authors are asked to send the "Copyright Transfer Agreement" to JSAT. Manuscripts will be published only after receiving the signed Copyright Transfer Agreement.

6. Publication or processing fee

No publication charge or processing fee.


JSAT
https://www.tci-thaijo.org/index.php/JSAT